Stem Cell Reports
Article

ISSCR

OPEN ACCESS

ESC-Derived BDNF-Overexpressing Neural Progenitors Differentially Promote Recovery in Huntington's Disease Models by Enhanced Striatal Differentiation

Tina Zimmermann,[1] Floortje Remmers,[1] Beat Lutz,[1] and Julia Leschik[1,*]
[1]Institute of Physiological Chemistry, University Medical Center, Johannes Gutenberg University, Duesbergweg 6, 55128 Mainz, Germany
*Correspondence: leschik@uni-mainz.de
http://dx.doi.org/10.1016/j.stemcr.2016.08.018

SUMMARY

Huntington's disease (HD) is characterized by fatal motoric failures induced by loss of striatal medium spiny neurons. Neuronal cell death has been linked to impaired expression and axonal transport of the neurotrophin BDNF (brain-derived neurotrophic factor). By transplanting embryonic stem cell-derived neural progenitors overexpressing BDNF, we combined cell replacement and BDNF supply as a potential HD therapy approach. Transplantation of purified neural progenitors was analyzed in a quinolinic acid (QA) chemical and two genetic HD mouse models (R6/2 and N171-82Q) on the basis of distinct behavioral parameters, including CatWalk gait analysis. Explicit rescue of motor function by BDNF neural progenitors was found in QA-lesioned mice, whereas genetic mouse models displayed only minor improvements. Tumor formation was absent, and regeneration was attributed to enhanced neuronal and striatal differentiation. In addition, adult neurogenesis was preserved in a BDNF-dependent manner. Our findings provide significant insight for establishing therapeutic strategies for HD to ameliorate neurodegenerative symptoms.

INTRODUCTION

The neurodegenerative disease Huntington's disease (HD) is characterized by dramatic motor dysfunction, cognitive decline, and psychiatric symptoms, which lead to progressive dementia and death approximately 15–20 years after onset (Landles and Bates, 2004). HD is an autosomal dominant inheritable disease, caused by mutations in the huntingtin (*HTT*) gene, leading to an increased number of polyglutamine repeats in the encoded protein (McMurray, 2001). How mutant HTT protein causes neuronal dysfunction and neurodegeneration has not yet been understood in detail, and besides the existence of some symptomatic treatments, so far there is no causal therapy available for patients. Numerous laboratories showed that in a large number of HD mouse models BDNF or BDNF/TRKB signaling is strongly reduced due to a mutant htt-mediated mechanism (Plotkin et al., 2014; Zuccato and Cattaneo, 2009). Besides causing changes in vesicular transport of BDNF (Gauthier et al., 2004), mutant HTT has been described to cause transcriptional downregulation of the BDNF gene through translocation of RE1 silencing transcription factor to the nucleus (Buckley et al., 2010). In addition to HD mouse models, a systematic and quantitative assessment of BDNF levels in human cerebral cortex samples, examined post mortem, confirmed that the production of this neurotrophin was impaired in the brains of HD patients (Zuccato et al., 2008). As striatal medium spiny neurons (MSNs) depend on BDNF activity, a number of studies attempted striatal neuroprotection by providing exogenous BDNF delivered to the diseased rodent striatum either by adenoassociated viral transfer or by transplantation of diverse genetically modified cell types (e.g., fibroblasts) (Connor et al., 2016; Sari, 2011). Altogether these studies showed enhanced neuroprotection, but no or only mild effects on long-term functional improvement in HD rodent models. On the other hand, cell transplantation as a promising therapeutic strategy, which aims to replace striatal neurons, has yielded some preliminary, but only modest and short-lived clinical benefits when using fetal neural cells (Bachoud-Levi et al., 2006; Gallina et al., 2010). Therefore, specifically embryonic stem cells (ESCs) and induced pluripotent stem cells (iPSCs) are considered to be an appropriate cell source, as ESCs can be differentiated in vitro into an MSN-like phenotype (Aubry et al., 2008; Danjo et al., 2011; Ma et al., 2012; Shin et al., 2012). However, their long-term survival, long-term functional improvement, and safety in vivo still need to be proved.

In the present study, we aimed to establish a combination therapy approach composed of cellular replacement by ESC-derived neural progenitors linked to BDNF supply. For this reason, we have generated BDNF-overexpressing mouse ESCs by knockin technology that display an enhanced neuronal and GABAergic differentiation in vitro (Leschik et al., 2013). Very recently, we were able to show that polysialylated neuronal cell adhesion molecule (PSA-NCAM)-positive progenitors derived from these ESCs lead to functional improvement when transplanted into mice with contusion spinal cord injury (Butenschön et al., 2016). With small modifications to the published protocol, which comprises magnetic-activated cell sorting (MACS) technology for purification, we tested in this study

the efficiency and safety in three divergent HD mouse models. At present, a variety of different HD mouse models exist, chemically or genetically induced, which match with some aspects of HD. However, until now none of them perfectly recapitulates human neuropathological hallmarks as well as progressive cognitive and motor impairments. So far, genetic HD mouse models have been used only in a few cell transplantation studies. In most cases, cell transplantation was performed in toxin-lesioned mice, in which vast neurodegeneration occurs. This is clearly an advantage over genetic mouse models, which harbor less neurotoxicity. In contrast, genetic accuracy is missing in toxin-induced lesions and it is therefore questionable whether this represents an appropriate model system to test therapeutics for human pathology. For this reason, we decided to use besides the toxin-lesioned model with quinolinic acid (QA) the two widely used transgenic mouse lines R6/2 and N171-82Q, which differ in their extent of pathological features and degree of impairment (Ramaswamy et al., 2007). Typical behavioral assays for each HD mouse model were chosen based on previous publications. We also included the automated gait analysis system CatWalk as a very sensitive method for measuring subtle changes in motor behavior. Here, we show that the CatWalk assay is a valid method to address motor behavior in the QA-lesion and N171-82Q mouse models. Cell transplantation with purified BDNF-expressing neural progenitors revealed an improved motor function in QA-lesioned mice, whereas only subtle effects on motor behavior were detected in both transgenic mouse lines. Therapeutic effects of BDNF-expressing progenitors in the QA model could be attributed to enhanced neuronal and striatal in vivo differentiation compared with control cells. Furthermore, tumor formation was completely absent, in contrast to other studies (Aubry et al., 2008).

RESULTS

Efficient In Vitro Preparation and Purification of Neural Precursor Cells for Transplantation

Mouse ESCs either overexpressing BDNF-GFP or GFP as control were differentiated as described previously via an embryoid body protocol followed by neural lineage selection (Butenschön et al., 2016). Cells were enriched for the intermediate neural progenitor marker PSA-NCAM and depleted of undifferentiated ESCs positive for stage-specific embryonic antigen-1 (SSEA-1) by MACS (Figure 1A). Cells were replated, and differentiation was induced by removal of basic fibroblast growth factor. Three days later, cells were analyzed by staining for multiple markers to ensure that BDNF-GFP and GFP cells were in the same stage of differentiation prior to transplantation (Figures 2A and 2B). Cultured cells (n = 3 independent experiments) expressed the neural stem cell markers Nestin (20.9% ± 3.2% BDNF-GFP, 23.9% ± 1.4% GFP cells) and PSA-NCAM (76.2% ± 4.4% BDNF-GFP and 65.4% ± 3.1% GFP cells). Only 1.5% ± 0.6% of BDNF-GFP and 2.5% ± 0.7% of GFP cells were positive for doublecortin (DCX). All neural progenitors expressed forkhead box protein G1 (FOXG1), one of the earliest markers of the telencephalic lineage. Few cells expressed the neuronal marker microtubule-associated protein 2 (MAP2) (1.3% ± 0.3% BDNF-GFP and 1.2% ± 0.1% GFP) and the astrocytic marker glial fibrillary acidic protein (GFAP) (1.3% ± 0.3% BDNF-GFP and 2.8% ± 0.6% GFP), whereas no cells expressed the oligodendrocytic marker oligodendrocyte transcription factor 2 (OLIG2). A fraction of proliferating cells was detectable by the M-phase marker KI67 (14.1% ± 1.2% BDNF-GFP and 10.9% ± 0.2% GFP neural progenitor cells [NPCs]), but all cells were positive for 5-bromo-2′-deoxyuridine (BrdU) (Figure 2C). No significant differences for any marker were detected between the two groups of cells. In vitro, BDNF-GFP cells were detectable with GFP immunostaining (Figure 2D) and showed BDNF-GFP-positive vesicles, while GFP NPCs displayed a uniform staining of the whole cell. As already shown in Butenschön et al. (2016), BDNF-GFP signal was barely detectable in vivo. Therefore, BrdU was used to label cells for transplantation, which was carried out in three different HD mouse models: QA lesion, R6/2, and N171-82Q. Figure 1B depicts the experimental outline of the transplantation studies with subsequent behavioral assays.

BDNF-GFP Cells Induce Locomotor Recovery in QA-Lesioned Mice

First, we addressed the functional effect of transplanting BDNF-GFP NPCs into the chemical HD mouse model with QA-induced lesion. Therefore, NPCs were transplanted at an animal age of 10 weeks, and groups (n = 10/group) were tested every other week for apomorphine-induced rotations (see experimental outline in Figure 1B). Immediately prior to transplantation, animals of all QA-lesioned groups displayed similar numbers of net rotations, which were significantly different from those mice that had only received a PBS injection instead of QA ($p < 0.001$).

After transplantation and repeated testing over time, QA-lesioned animals (QA + Hank's balanced salt solution [HBSS], QA + GFP NPCs, and QA + BDNF-GFP NPCs) exhibited significantly higher net rotations at all time points compared with non-lesioned animals (PBS + HBSS) (Figure 3A). Recovery became significant 8 weeks after transplantation, when animals in the BDNF-GFP transplant group displayed 85 ± 22.65 net rotations compared with 132.6 ± 19.84 in the QA-HBSS group ($p = 0.005$) (Figure 3B). GFP cell-transplanted animals did not display significant

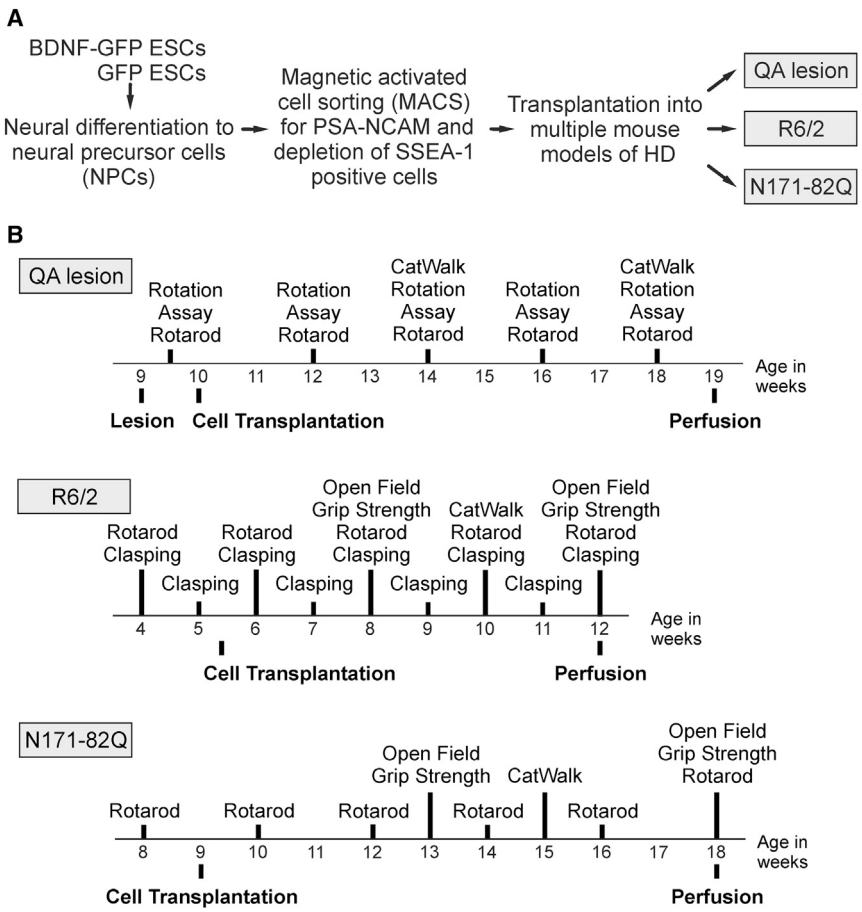

Figure 1. Experimental Outline of the Study

(A) General concept. BDNF-GFP and GFP ESCs were differentiated to NPCs and sorted by MACS for a PSA-NCAM$^+$/SSEA-1$^-$ population. After 3 days of differentiation, cells were transplanted into the striatum of three different HD mouse models: the QA-lesioned, R6/2, and N171-82Q mouse models.

(B) Overview of mouse models and respective behavioral assays at distinct time points of age.

improvement of locomotor function compared with control animals (QA + HBSS) 8 weeks after transplantation (Figure 3B).

Rotarod data showed similar results, with BDNF-GFP cells improving motor function of QA-lesioned mice (Figure 3C). Mice with BDNF-GFP transplants improved in their latency to fall and were not significantly different ($p = 0.144$) when compared with non-lesioned control animals during repeated testing. In contrast, GFP transplants did not ameliorate motor function over time, as they still differed significantly from the non-lesioned control group, with $p = 0.022$ during repeated testing. However, when looking at a single time point at 18 weeks of age (8 weeks after transplantation), the mean latency of 153.2 ± 13.61 s detected for the GFP cell-transplanted group did not significantly differ any longer from non-lesioned control animals (PBS + HBSS; 202.8 ± 13.31 s latency) (Figure 3D). This means that also GFP cells exerted a significant functional recovery, which was similar to the improvement of BDNF-GFP cell-transplanted animals at 8 weeks after transplantation, as no significant difference between both groups was detected. Only HBSS vehicle-treated QA-animals still displayed significantly lower motor performance than the healthy control group ($p = 0.023$).

In addition to the analysis of motor performance by the rotation and Rotarod assays, we established the use of the CatWalk gait system in the QA-lesion HD model. Figure S1 graphically demonstrates distinct gait parameters, which were significantly affected in QA-lesioned mice compared with non-lesioned control animals, and Table S1 presents quantitative data of these gait parameters. At 14 weeks of age, QA-lesioned mice displayed significantly reduced walk speed (PBS + HBSS 282.4 ± 16.2 mm/s, QA + HBSS 225.3 ± 7.4 mm/s; $p = 0.009$) and swing speed (e.g., PBS + HBSS[left forepaw, LF] 623.7 ± 25.9 mm/s, QA + HBSS[LF] 534.7 ± 14.0 mm/s; p[LF] = 0.038) and enhanced swing (e.g., PBS + HBSS[left hindpaw, LH] 0.1095 ± 0.0032 s, QA + HBSS[LH] 0.1215 ± 0.0030 s; p[LH] = 0.018) compared with non-lesioned control mice. At 18 weeks of age, additionally cadence (PBS + HBSS 18.6 ± 0.86 steps/s, QA + HBSS 15.11 ± 0.62 steps/s; $p = 0.005$) and stride length (e.g., PBS + HBSS[right forepaw, RF] 81.28 ± 0.80 mm, QA + HBSS[RF] 67.13 ± 1.19 mm; p[RF] = 0.0001) were significantly reduced, whereas stand (e.g., PBS + HBSS[RF]

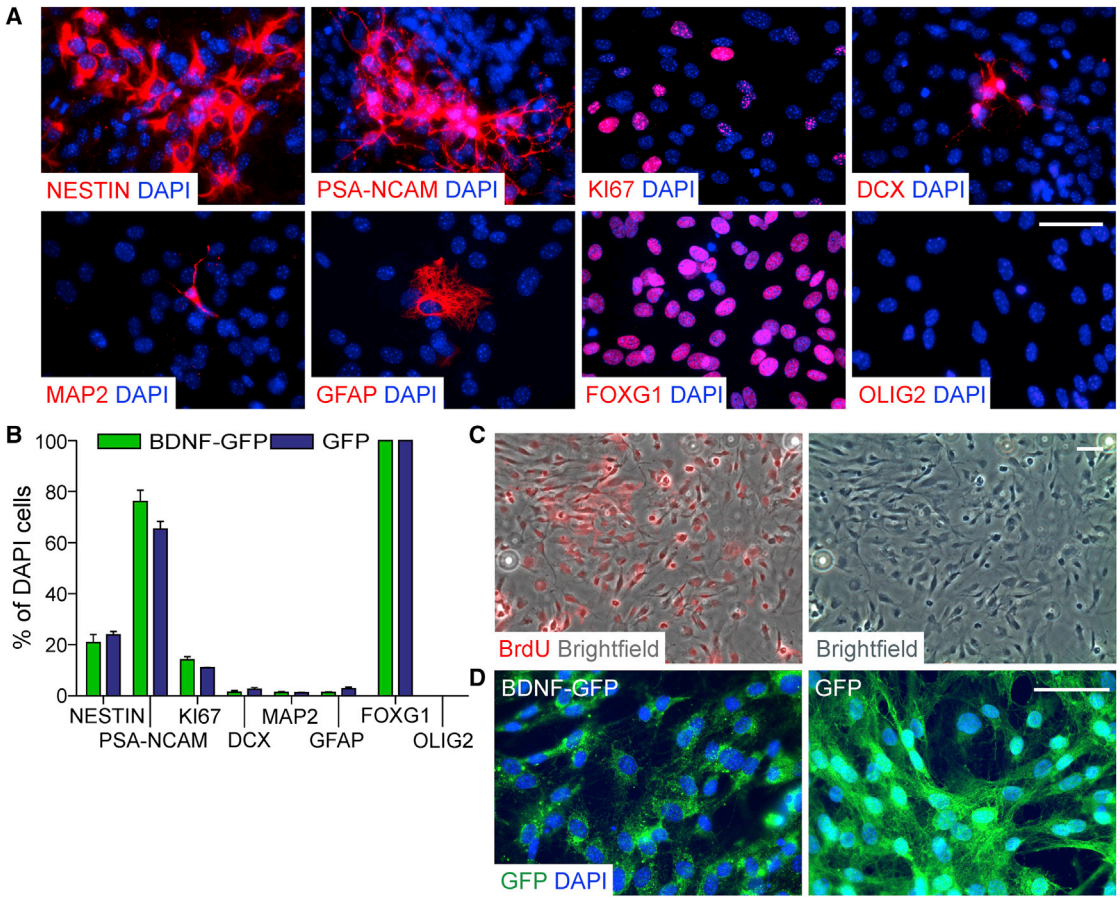

Figure 2. BDNF-GFP and GFP Cells Do Not Differ in Expression of Neural, Glial, and Neuronal Markers before Transplantation

(A) Generation of NPCs was analyzed after 3 days of differentiation after MACS by immunostaining for NESTIN, PSA-NCAM, KI67, DCX, MAP2, GFAP, FOXG1, and OLIG2 (BDNF-GFP cells, all stained in red).

(B) Respective percentages of marker expression of all DAPI cells. No significant difference ($p = 0.3656$) between BDNF-GFP and GFP cells was detected ($n = 3$ independent experiments).

(C) Overlay of fluorescent and bright-field microscopic images demonstrates that all cells were labeled with BrdU and hence proliferative.

(D) Anti-GFP immunocytochemistry of purified BDNF-GFP NPCs shows the vesicular distribution of BDNF throughout the cell, whereas in GFP NPCs, GFP is detected in the whole cytoplasm.

Scale bars, 50 μm.

0.1079 ± 0.0047 s, QA + HBSS[RF] 0.1440 ± 0.0057 s; p[RF] = 0.001) and duty cycle (e.g., PBS + HBSS[RF] 51.60% ± 0.51%, QA + HBSS[RF] 55.60% ± 0.47%; p[RF] = 0.001) was significantly enhanced. Figure 3E further demonstrates qualitatively in tabular representation which gait parameters of which paw could be partially rescued by either or both types of NPCs. In general, measuring at 14 weeks of age (4 weeks after transplantation) seemed to be more effective than at a later time point. Here, swing (QA + GFP NPCs[LH] 0.1201 ± 0.0027 s, p[LH] versus PBS + HBSS[LH] = 0.057) and swing speed (e.g., QA + GFP NPCs[LF] 582.00 ± 31.69 mm/s, p[LF] versus PBS + HBSS[LF] = 0.109, QA + BDNF-GFP NPCs[LF] 546.59 ± 19.60 mm/s, p[LF] versus PBS + HBSS[LF] = 0.596) were improved by either GFP cells alone or both cell types, which was no longer measurable at 18 weeks of age. At this time point, only duty cycle was positively affected by GFP and BDNF-GFP NPCs (QA + GFP NPCs 55.05% ± 3.54%, p versus PBS + HBSS = 0.088; QA + BDNF-GFP NPCs 54.97% ± 3.05%, p versus PBS + HBSS = 0.100).

CatWalk Gait Parameters of the R6/2 Model Are Affected by Transplantation of NPCs

Next, we asked how transplantation of NPCs affects pathology in the transgenic R6/2 mouse model of HD. The middle panel of Figure 1B describes the experimental outline with cell transplantation into R6/2 animals (n = 10–12/group) at 5 weeks of age and consecutive behavioral assays until the

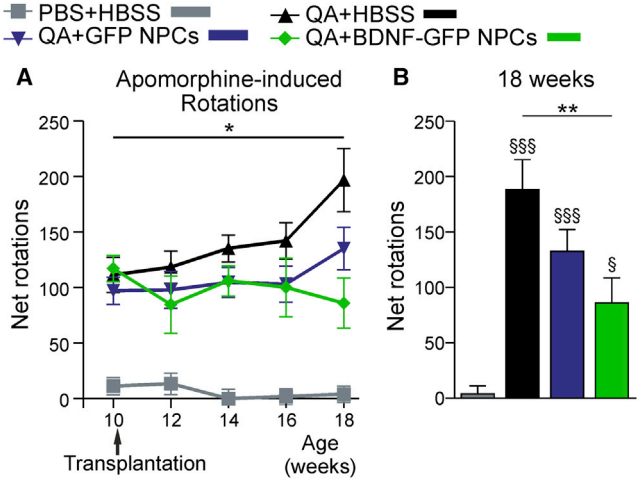

E CatWalk

parameters significantly different between QA- and non-lesioned		paw: partial rescue by NPCs
14 weeks	Walk speed	-
	Swing	LH: GFP
	Swing speed	LF: GFP, BDNF-GFP LH: GFP
18 weeks	Walk speed	-
	Swing	-
	Swing speed	-
	Cadence	-
	Stride length	-
	Stand	-
	Duty Cycle	RH: GFP, BDNF-GFP

Figure 3. BDNF-GFP Cells Improve Locomotor Function in QA-Lesioned Mice 8 Weeks after Transplantation

(A) Analysis of rotational behavior in response to apomorphine. At all time points, non-lesioned animals (PBS + HBSS) displayed significantly fewer rotations (*$p < 0.05$) than QA-lesioned (QA + HBSS, QA + GFP NPCs, and QA + BDNF-GFP NPCs) animals.

(B) At an age of 18 weeks (8 weeks after transplantation), all lesioned groups were different from the non-lesioned group (QA + HBSS: $p < 0.001$; QA + GFP NPCs: $p < 0.001$; QA + BDNF-GFP NPCs: $p = 0.03$). However, BDNF-GFP NPCs showed a highly significant decrease in net rotations compared with untreated, lesioned animals (**$p = 0.005$). Values represent mean ± SEM; $^{§§§}p < 0.001$, $^{§}p < 0.05$ versus PBS + HBSS.

(C) Analysis of motor behavior on the Rotarod. An overall group effect was observed ($p = 0.006$), without a significant interaction for cell groups × time ($p = 0.076$). BDNF-GFP NPCs did not differ from non-lesioned animals ($p = 0.144$), but GFP NPC-grafted ($p = 0.022$) and non-grafted animals ($p = 0.009$) were significantly different from non-lesioned animals. *$p < 0.05$, ***$p < 0.001$.

(D) Analysis of Rotarod performance at an age of 18 weeks (8 weeks after transplantation). Only lesioned, non-grafted animals were significantly different to non-lesioned mice ($p = 0.023$), showing a beneficial effect of transplanted cells on Rotarod performance. *$p < 0.05$ versus PBS + HBSS.

(E) List of affected CatWalk gait parameters, analyzed by one-way ANOVA with post hoc Tukey's test between groups for each paw. At 14 weeks of age, the following parameters were significantly different ($p < 0.05$) between lesioned and non-lesioned animals: walk speed, swing, and swing speed. NPCs affected beneficially swing and swing speed. At 18 weeks of age, the following parameters were additionally significantly different: cadence, stride length, stand, and duty cycle. RH, right hindpaw; LF, left forepaw; LH, left hindpaw.

Data represent mean (n = 10 animals) ± SEM. For explanatory graphs and statistics, see Figure S1.

age of 12 weeks. Rotarod and hindlimb clasping, the two mainly used assays for functional assessment of the R6/2 line, revealed no differences between NPC-transplanted animals and vehicle control R6/2 animals (Figures 4A and 4B). Similar results were obtained with the grip strength and open field test. Only the wild-type (WT) group behaved significantly different compared with the transplanted and non-transplanted R6/2 groups (Figures 4C and 4D). Furthermore, body weight, an increase of which can be taken as a measure of physical recovery, was unchanged between R6/2 groups (Figure 4E). However, when we tested animals in the CatWalk gait system, we detected functional improvements in certain parameters after cell transplantation. Partial rescue effects in stride length (e.g., WT[LF] 80.46 ± 1.22 mm, transgenic [TG][LF] 71.18 ± 2.59 mm; p[LF] = 0.014) were detected in animals that had received GFP (LF 74.74 ± 1.36 mm, p[LF] versus WT = 0.231) or BDNF-GFP (LF 72.97 ± 2.54 mm, p[LF] versus WT = 0.071) cell transplants. In contrast, lateral support (WT 0.55% ± 0.36%, TG 5.67% ± 1.94%, p = 0.041) was partially rescued only by BDNF-GFP cells (5.43% ± 1.47%, p versus WT = 0.064) (Figure 4F and Table S2).

Transplantation of NPCs into the N171-82Q Mouse Model Exerts Beneficial Effects in the CatWalk Test

Similar to cell transplantation into R6/2 mice, the robust Rotarod assay as well as the grip strength test revealed no differential effects by transplanted NPCs compared with vehicle-injected N171-82Q animals (n = 10–12/group) (Figures 5A and 5B; experimental outline Figure 1B, lower panel). Furthermore, the lack of body weight gain in transgenic animals could not be rescued (Figure 5D) and the open field test did not result in significant reduction of

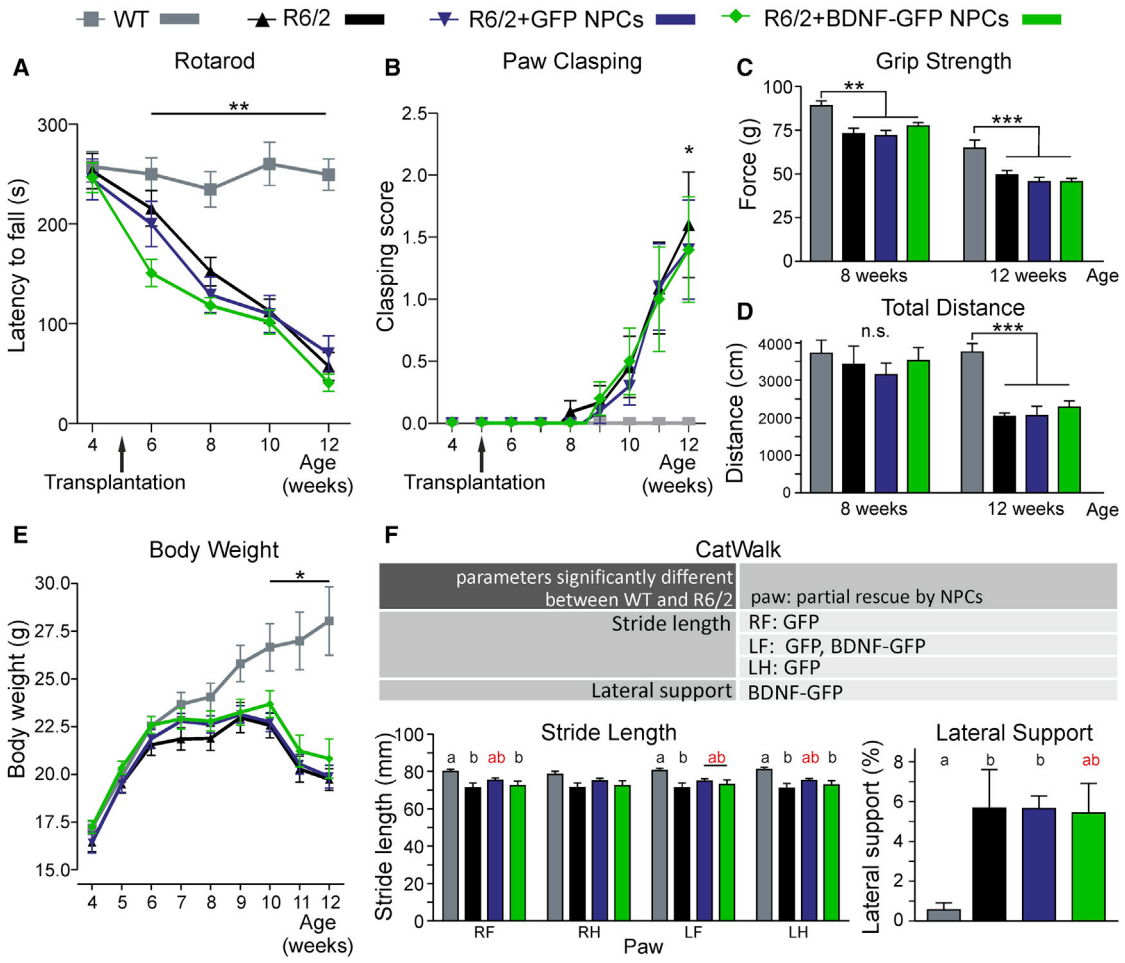

Figure 4. Few Gait Parameters of the R6/2 Model Are Affected by Transplantation of NPCs

(A) Behavioral performance on the Rotarod was assessed every 2 weeks. R6/2 mice show significantly lower latency to fall from the Rotarod compared with wild-type (WT) mice after transplantation starting at 6 weeks of age (**$p < 0.01$). No effect of transplanted NPCs on transgenic R6/2 mice was observed at any time point.

(B) Paw clasping was analyzed weekly. R6/2 mice had a significantly higher clasping score compared with WT animals at 12 weeks of age. Cell transplantation did not have any effect on performance in the paw-clasping test.

(C) Grip strength of WT and R6/2 mice was measured at 8 and 12 weeks of age. Non-treated and grafted R6/2 mice displayed a significant decrease in grip strength at both time points. No effect of transplanted NPCs was observed.

(D) Quantification of total distance of WT and R6/2 mice in the open field.

(E) Body weight was measured weekly. ANOVA with repeated measures (cell groups × time, $p = 0.001$) and consecutive simple effects analysis with Sidak correction show a significant decrease of body weight in all transgenic R6/2 compared with WT animals from 10 weeks of age on.

(F) Gait parameters of R6/2 mice were analyzed on the CatWalk at 10 weeks of age, revealing differences in stride length and lateral support. Stride length of R6/2 mice was partially rescued by transplantation of NPCs, except for the right hindpaw. Lateral support of R6/2 mice was partially decreased when BDNF-GFP NPCs were transplanted. Values of bars with a different letter (a or b) were significantly different ($p < 0.05$) from each other. Values of bars with the same letter (a or b) were not significantly different from each other, hence values of bars marked with "ab" (marked in red) are not significantly different from either a or b, which indicates a partial/incomplete rescue of the phenotype. RF, right forepaw; RH, right hindpaw; LF, left forepaw; LH, left hindpaw.

Data represent mean (n = 10–12 animals) ± SEM; *$p < 0.05$, **$p < 0.01$, ***$p < 0.001$ versus WT; n.s., not significant.

moved distance in transgenic compared with WT animals (Figure 5C). Hence, a visible improvement due to NPC transplantation was not detectable.

To identify the occurrence of more subtle motoric effects after cell transplantation, we also established the CatWalk gait system for the analysis of the N171-82Q mouse line.

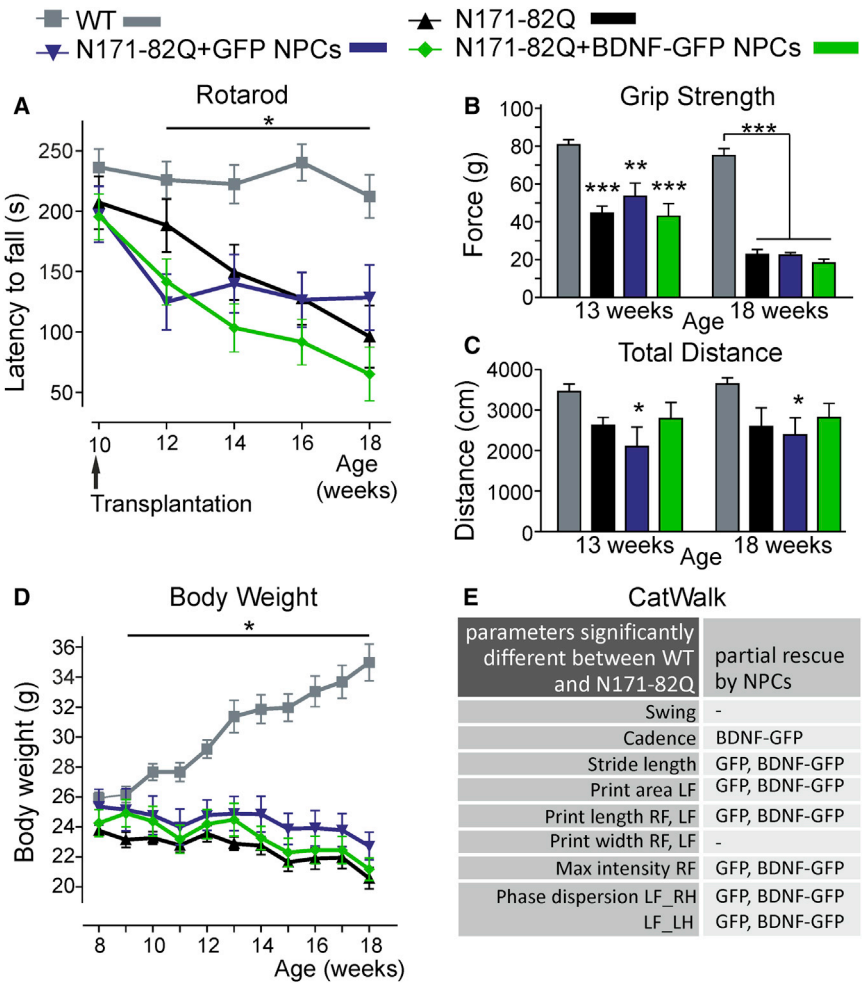

E CatWalk

parameters significantly different between WT and N171-82Q	partial rescue by NPCs
Swing	-
Cadence	BDNF-GFP
Stride length	GFP, BDNF-GFP
Print area LF	GFP, BDNF-GFP
Print length RF, LF	GFP, BDNF-GFP
Print width RF, LF	-
Max intensity RF	GFP, BDNF-GFP
Phase dispersion LF_RH	GFP, BDNF-GFP
LF_LH	GFP, BDNF-GFP

Figure 5. Transplantation of NPCs into the N171-82Q Mouse Model Exerts Beneficial Effects in the CatWalk Test

(A) Analysis of motor behavior on the Rotarod. N171-82Q mice showed a significant decrease in the latency to fall compared with WT animals from 12 weeks of age on. No difference between NPC-transplanted and non-transplanted mice was detected.

(B) Grip strength of transgenic animals was not influenced by transplantation of NPCs at 13 or 18 weeks of age, but was lower than in WT.

(C) Total distance moved in the open field was not changed in transgenic animals compared with WT mice at 13 or 18 weeks of age. Transplantation of GFP NPCs in transgenic N171-82Q animals reduced the distance moved at both time points compared with WT mice, but had no effect when compared with transgenic N171-82Q mice.

(D) Weekly body weight measurement showed a slow loss of body weight in transgenic animals, whereas WT mice gained body weight over time (ANOVA with repeated measures [cell groups × time, $p = 0.001$] and consecutive simple effects analysis with Sidak correction) from 9 weeks of age on. No difference was detected between transplanted and non-transplanted animals.

(E) Overview of different gait parameters as quantified by the CatWalk test ($p < 0.05$). NPCs affected positively altered cadence, stride length, print area, print length, maximum intensity of distinct paws, and phase dispersion. For explanatory graphs and statistics, see Figure S2. RF, right forepaw; RH, right hindpaw; LF, left forepaw; LH, left hindpaw.

Data represent estimated marginal mean (A) or mean (B–D) (n = 10–12 animals) ± SEM; *$p < 0.05$, **$p < 0.01$, ***$p < 0.001$ versus WT; n.s., not significant.

Indeed, we uncovered many gait parameters, which were significantly different in N171-82Q transgenic and WT mice (Figure S2 and Table S2). Affected gait parameters were cadence (WT 26.41 ± 1.75 steps/s, TG 32.59 ± 1.50 steps/s; $p = 0.031$), swing (e.g., WT[RF] 0.0761 ± 0.0027 s, TG[RF] 0.0605 ± 0.0019 s; $p = 0.0001$), stride length (e.g., WT[RF] 88.37 ± 3.39 mm, TG[RF] 73.54 ± 2.82 mm; p[RF] = 0.01), print area (WT[LF] 24.85 ± 0.98 mm^2, TG [LF] 20.74 ± 1.32 mm^2; $p = 0.047$), print length (e.g., WT [RF] 8.54 ± 0.18 mm, TG[RF] 7.79 ± 0.19 mm; p[RF] = 0.028), print width (e.g., WT[RF] 8.09 ± 0.14 mm, TG[RF] 6.64 ± 0.24 mm; p[RF] = 0.001), maximum intensity (WT [RF] 50.14 ± 1.29 a.u., TG[RF] 35.95 ± 2.11 a.u.; p[RF] = 0.001), and phase dispersion (e.g., WT[LF_right hindpaw, RH] 3.89% ± 1.24%, TG[LF_RH] 11.43% ± 1.72%; p[LF_RH] = 0.009). This demonstrates that the CatWalk can be used as a valid system to address motor function in the N171-82Q mouse line. With this method changes of defined motoric parameters due to NPC transplantation were detected. These are summarized in tabular representation (Figure 5E; for explanatory graphs and statistics see Figure S2 and Table S2). Most of the parameters—stride length (e.g., TG + GFP NPCs [RF] 80.46 ± 1.68 mm, p[RF] versus WT = 0.359; TG + BDNF-GFP NPCs [RF] 77.02 ± 3.71 mm, p[RF] versus WT = 0.058), print area (TG + GFP NPCs [LF] 22.16 ± 1.04 mm^2, p[LF] versus WT = 0.359; TG + BDNF-GFP NPCs [LF] 22.26 ± 1.01 mm^2, p[LF] versus WT = 0.304), print length (e.g., TG + GFP NPCs [RF] 8.04 ± 0.22 mm, p[RF] versus WT = 0.286; TG + BDNF-GFP NPCs [RF] 8.32 ± 0.17 mm, p[RF] versus WT = 0.816), phase dispersion (e.g., TG + GFP NPCs [LF_RH] 8.56% ± 1.39%, p[LF_RH] versus WT = 0.222; TG + BDNF-GFP NPCs

[LF_RH] 8.57% ± 1.92%, p[LF_RH] versus WT = 0.151)—were partially rescued by both NPC types, and no significant difference between transplantation with GFP and BDNF-GFP cells was measured. However, cadence was only positively affected after transplantation with BDNF-GFP NPCs (TG + BDNF-GFP NPCs 31.70 ± 1.53 steps/s, p versus WT = 0.069).

Cell Survival Is Differentially Altered in NPC-Transplanted Groups in the Three Mouse Models

Stereotaxic injection of QA into the striatum of C57BL/6J mice led to an almost complete depletion of MSNs positive for dopamine- and cyclic AMP-regulated neuronal phosphoprotein (DARPP32) (Figure 6A). The lesion volume did not differ between the groups (QA + HBSS 1.13 ± 0.13 mm^3, QA + GFP NPCs 1.09 ± 0.16 mm^3, and QA + BDNF-GFP NPCs 1.17 ± 0.28 mm^3, Figure 6B, n = 4/group). Differentiated ESCs injected into the lesion center 1 week after lesioning were detected by BrdU staining (Figure 6C) and, most importantly, showed no sign of tumor formation. The initial graft contained 100,000 cells, and stereological estimation (n = 4/group) revealed that 20.10% ± 4.51% BDNF-GFP and 21.65% ± 2.98% GFP NPCs survived 9 weeks after transplantation in the striatum (Figure 6D). No significant differences were detected between both transplantation groups. Additionally we investigated cellular survival for the two genetic mouse models. Cell survival in the transgenic R6/2 model (Figure 6E, n = 4/group) was lower than in the QA model; 9.61% ± 2.96% BDNF-GFP and 9.78% ± 1.48% GFP cells survived after transplanting 100,000 cells/hemisphere. In contrast, quantification of transplanted cells in the transgenic N171-82Q model (Figure 6F, n = 4/group) shows that 17.89% ± 1.09% BDNF-GFP cells and 10.65% ± 2.52% survived. Here, cell survival was increased when transplanting BDNF-GFP cells (p = 0.039). In both transgenic mouse lines (Figures 6G and 6H), BDNF-GFP cells produce BDNF as detected by BDNF-antibody staining. Under high magnification, BDNF-GFP can also be detected with the GFP antibody, albeit at an almost undetectable level (Figure 6H). In contrast, GFP cells are only positive for GFP without showing BDNF expression (Figures 6G and 6H).

BDNF-GFP NPCs Differentiate Preferably Toward Neuronal Cell Fate in the QA-Lesioned Striatum and Influence Endogenous Neurogenesis

QA-induced lesion was the only HD mouse model that exhibited a robust functional improvement after injection of BDNF-GFP NPCs. For this reason, we analyzed positive NPC effects in detail to elucidate their mechanism of action. To determine the cell fate of transplanted cells, we double stained BrdU cells (n = 8 animals/group) with antibodies against the three neural cell lineages (Figure 7A). Figure 7B shows that 9 weeks after transplantation, the number of BrdU-positive neurons was significantly higher (p = 0.0446) in BDNF-GFP grafts (MAP2, 56.14% ± 3.83%) than in GFP grafts (45.88% ± 2.74%). In contrast, the number of corresponding $S100B^+$ astrocytes (BDNF-GFP 32.29% ± 1.63%, GFP 47.57% ± 6.77%) was decreased (p = 0.0486). This means that BDNF-GFP NPCs favor neuronal ($MAP2^+$) over astrocytic ($S100B^+$) differentiation (p = 0.0001). Only few aspartoacylase (ASPA)-positive oligodendrocytes were observed in BDNF-GFP grafts (1.29% ± 0.18%), but fewer (p = 0.0015) than in GFP grafts (5.50% ± 0.96%). BDNF-GFP NPCs differentiated strikingly (p = 0.0022) into the striatal lineage, as assessed by staining for the striatal specific transcription factor forkhead box protein (FOXP1) (BDNF-GFP graft 42.67% ± 3.55%, GFP graft 24.00% ± 3.22%). Analysis of DCX immunolabeling showed no significant difference in the percentage of DCX-positive cells in BDNF-GFP (1.13% ± 0.79%) and GFP (5.25% ± 3.44%) grafts.

Endogenous neurogenesis in the dorsal subventricular zone (SVZ) was increased upon QA lesioning of the striatum, as evaluated by staining (n = 4 animals/group) for the neuronal precursor marker DCX (Figure 7C). Quantification of DCX numbers (Figure 7D) revealed a significant increase in the number of DCX cells of BDNF-GFP NPCs grafted (16,430 ± 1,567 cells) and non-grafted, lesioned (14,690 ± 2,327 cells) animals compared with healthy (8,335 ± 885 cells) animals. GFP NPC transplantation (13,210 ± 1,241 cells) did not significantly (p = 0.124) affect endogenous neural precursor proliferation.

DISCUSSION

Stem cell therapy and BDNF supply are two individual approaches for the treatment of HD. Given that a combination of both might be particularly promising, we tested the use of BDNF-overexpressing NPCs, which had been derived from mouse ESCs. We compared the functional outcome after transplantation into three different HD mouse models and observed robust motor improvements only in the QA toxin-induced lesion model of HD. In contrast, transplantation into both transgenic HD mouse models R6/2 and N171-82Q resulted only in minor general NPC effects.

The standard behavioral paradigm to test motor function in the QA model is the apomorphine-induced rotation assay, which tests the unilateral dysfunction of the striatum (Bernreuther et al., 2006; Ramaswamy et al., 2007). Furthermore, the Rotarod as a test for motor coordination and motor learning, which is widely used for QA-lesioned rats, has been also described for mice with QA lesion (Chiarlone et al., 2014). With both assays, we detected a functional

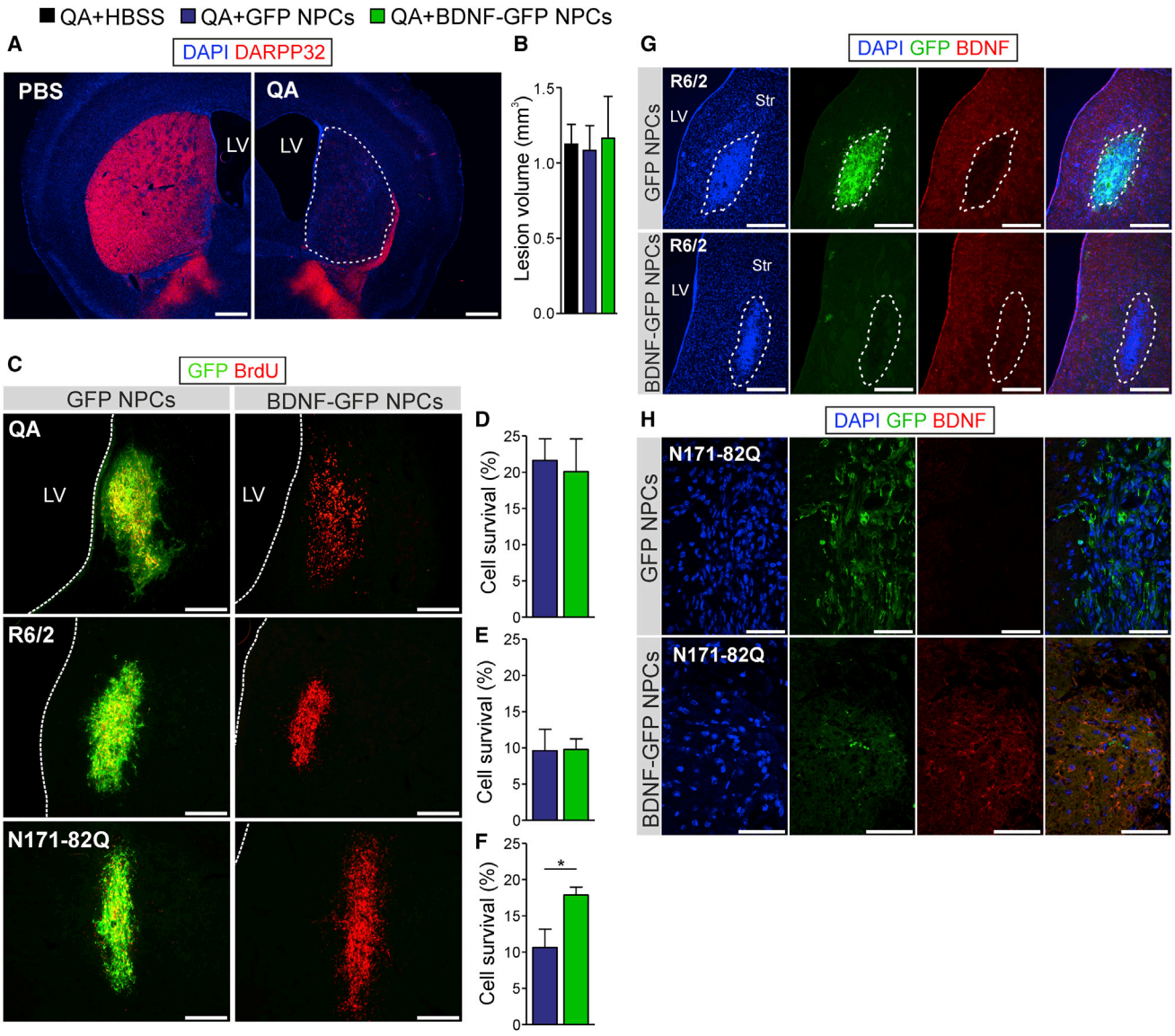

Figure 6. Detection of Grafted GFP and BDNF-GFP Expressing NPCs in the Striatum of Chemical and Transgenic HD Mice

(A) Representative photomicrographs of mouse brain sections from lesioned (QA) and non-lesioned (PBS) mice. Immunostaining for DARPP32 (red) showed that lesioning leads to a widespread loss of medium spiny neurons in the striatum. Dotted lines indicate lesioned area. Scale bars, 500 μm.

(B) Quantitative analysis showed that lesion volume does not differ ($p = 0.97$) between vehicle-treated and transplanted groups ($n = 4$ animals). Values are expressed as mean ± SEM.

(C–F) Representative micrographs for all three mouse models are shown in (C). GFP cells are positive for BrdU and showed robust GFP expression. However, GFP signal of BDNF-GFP expressing cells is very weak and almost undetectable by confocal microscopy, but cells could be efficiently traced by BrdU. Scale bars, 250 μm. Dotted lines indicate the lateral ventricle (LV). Graphs show quantification of cell survival ($n = 4$ animals) in the QA (D), the R6/2 (E), and N171-82Q (F) mouse models. Cell survival in the QA and R6/2 model is not different between BDNF-GFP and GFP transplanted cells, whereas in the N171-82Q model cell survival was significantly increased ($p = 0.039$) by transplanting BDNF-GFP cells. Data represent mean ± SEM; *$p < 0.05$.

(G and H) Grafts (dotted lines) of GFP and BDNF-GFP expressing NPCs (G) in the striatum (Str) of R6/2 mice 7 weeks after cell transplantation at low magnification (Scale bars, 250 μm), or (H) in N171-82Q mice 9 weeks after cell transplantation at higher magnification (Scale bars, 50 μm). Representative micrographs prove BDNF expression in BDNF-GFP NPCs with very weak detection of GFP signal at higher magnification (lower panels in G and H). In contrast, BDNF-signal was absent in GFP expressing cells (upper panels in G and H). LV, lateral ventricle.

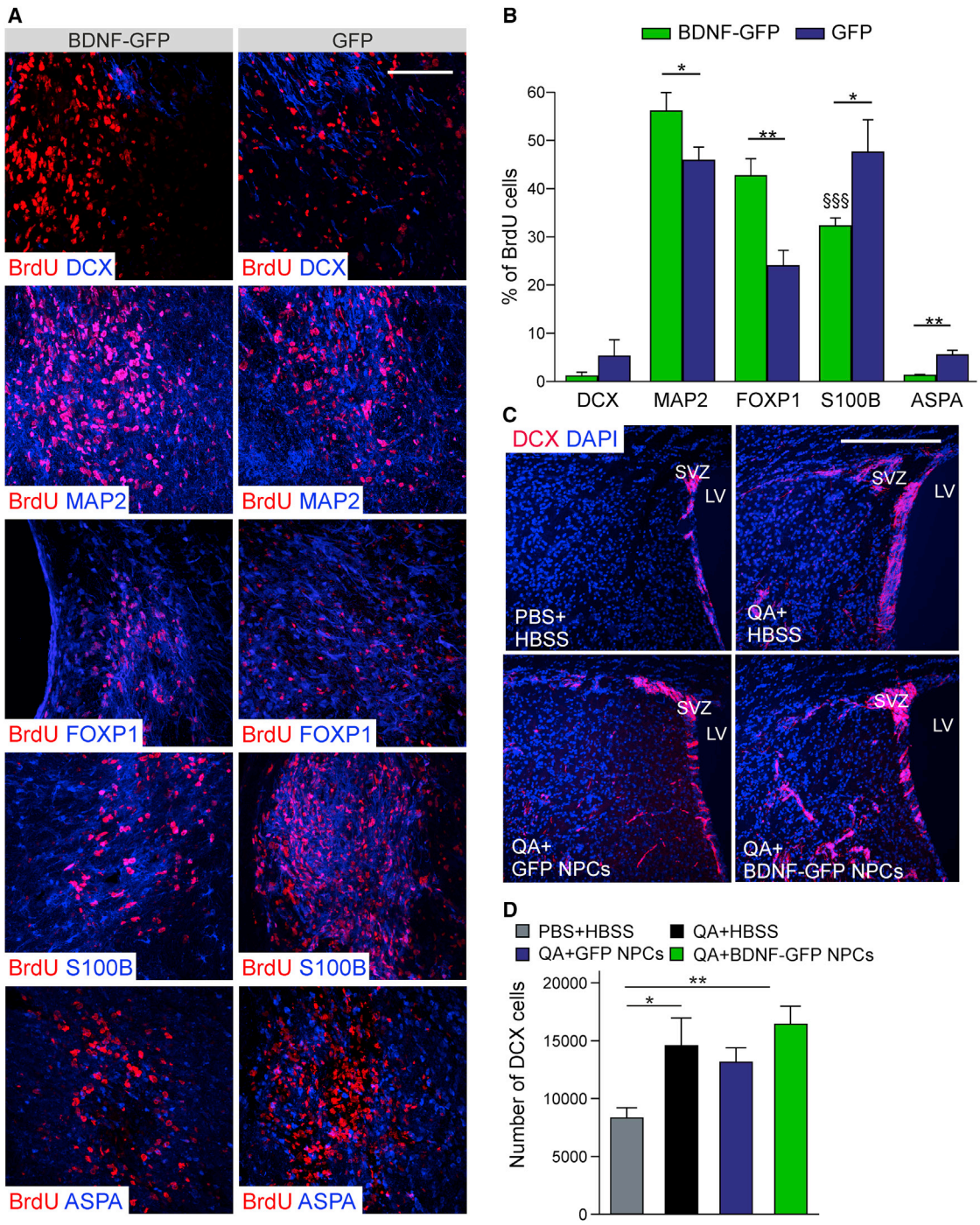

Figure 7. BDNF-GFP Cells Grafted into the QA-Lesioned Striatum Showed Enhanced Neuronal Differentiation and Preserved Adult Neurogenesis of the SVZ

(A) Maximum-intensity projections of confocal micrographs of BDNF-GFP and GFP grafted cells. Transplanted cells were detected with BrdU staining (red) and were positive for DCX, MAP2, FOXP1, S100B, and ASPA (all in blue). Scale bar, 100 μm.

(B) Corresponding counts of double-positive cells (n = 8 animals). BDNF-GFP cells differentiated significantly more into a neuronal ($MAP2^+$, $p = 0.0446$) and striatal ($FOXP1^+$, $p = 0.0022$) lineage compared with GFP cells, whereas GFP cells differentiated more into the glial ($S100B^+$, $p = 0.0486$ and $ASPA^+$, $p = 0.0015$) lineage compared with BDNF-GFP cells. In addition, BDNF-GFP cells favored highly significant neuronal ($MAP2^+$) differentiation over astrocytic ($S100B^+$) differentiation ($^{§§§}p = 0.0001$ versus BDNF-GFP MAP2). Values represent mean ± SEM; $^*p < 0.05$, $^{**}p < 0.01$.

(legend continued on next page)

improvement after transplantation of BDNF-GFP NPCs. Instead, GFP NPCs were only supportive when animals were tested in the Rotarod. Both types of NPCs exerted beneficial effects on evaluation of distinct CatWalk gait parameters. The CatWalk method is an automated, computerized gait analysis technique that allows objective analysis of very confined motor function. In HD research, it has so far only been described for the analysis of the R6/2 mouse model (Chiang et al., 2010) and HD transgenic rats (Vandeputte et al., 2010). Our data show that the CatWalk assay is also a valuable behavioral paradigm for the analysis of the QA-lesioned mouse model. Specific gait characteristics (walk and swing speed, swing, cadence, stride length, duty cycle) were significantly different in QA-lesioned and non-lesioned mice. Furthermore, we established the CatWalk gait system for the N171-82Q mouse model and were able to show that multiple gait parameters were significantly changed when comparing WT and transgenic mice. With this tool, we further identified functional improvements after transplanting NPCs into N171-82Q mice, which we were not able to detect with the Rotarod and grip strength tests. Therefore, we assume that the CatWalk system is a more sensitive assay for detection of subtle, but profound, well-defined motor functions, which can be related to patients' symptoms. Besides chorea, HD patients display a more general progressive deterioration of skilled movements, which may also affect essential motor skills such as manual dexterity, locomotion, and specific gait parameters (Foltstein et al., 1983; Koller and Trimble, 1985). The CatWalk test is able to detect these gait impairments in mice. Other behavioral measures, such as the Rotarod test, detect general coordination, especially chorea. With our transplant intervention, we were able to detect partial improvements in several gait parameters. However, due to small differences in absolute values between WT and transgenic animals, it was difficult to reveal intermediate improvements, such as those between BDNF-GFP and GFP transplants. In most gait parameters, both NPC types partially rescued the pathological phenotype, but effects were not different when comparing both transplant groups. However, cadence, as a single gait parameter, was only positively affected by BDNF-GFP cells in the N171-82Q mouse model. In contrast to N171-82Q mice, the R6/2 line behaved differently on the CatWalk, where only stride length and lateral support were significantly changed, which is in agreement with published data (Chiang et al., 2010). Both gait parameters could be partially rescued either by GFP or BDNF-GFP cells, or by both NPC types. In general, we did not detect a considerable improvement of functional recovery in the R6/2 mouse line, as the two vigorous behavioral paradigms Rotarod and paw clasping were unchanged.

One possible explanation for the differential behavioral improvements in the three distinct HD mouse models could be the different cell survival rate with the highest survival rate in QA-lesioned animals. NPCs transplanted into transgenic animals generally displayed lower cell survival, a phenomenon that has already been demonstrated in other publications (Ebert et al., 2010; El-Akabawy et al., 2012; Snyder et al., 2010), possibly due to the progressive pathology in transgenic mice. Particularly after transplantation into R6/2 animals, approximately only half of the cells compared with QA-lesioned animals were detectable. Transplantation into the N171-82Q mice resulted in an intermediate cell survival rate compared with both other mouse models. Interestingly, only in the N171-82Q mouse model we detected a difference in the cell survival rate of both NPC types. Here, BDNF-GFP cells survived better than GFP cells, which might explain why more gait parameters are significantly changed by BDNF-GFP NPCs compared with the R6/2 line. Furthermore, the different degree of survival may be explained by the fact that in the transgenic lines the absence of a lesion leads to a densely packed graft core, which might hinder survival, migration, and integration of grafted cells (Behrstock et al., 2008). Although transgenic mouse models are genetically more accurate and neurodegeneration is progressive, they still lack the feature of extensive neuronal cell death, which seems to be a prerequisite for survival and integration of transplanted cells (Labandeira-Garcia et al., 1991; Watts and Dunnett, 1998) Therefore, most of studies addressing cellular therapies for HD used QA-lesioned rodent models, which display massive and predictable cell loss (Aubry et al., 2008; Bernreuther et al., 2006; Ma et al., 2012; Shin et al., 2012). Only few cell transplantation studies with different types of stem or progenitor cells used transgenic HD mouse models and obtained minor or no motoric outcome. Especially with the R6/2 line, it was difficult to obtain any kind of improvement (El-Akabawy et al., 2012; Fink et al., 2013), whereas N171-82Q seemed to be the more appropriate transgenic model for cell transplantation (Ebert et al., 2010; Snyder et al., 2010). We can

(C) Representative sections through the SVZ of NPC-transplanted, vehicle-treated, and non-lesioned animals immunostained for DCX (red) and DAPI (blue). Scale bar, 200 μm.

(D) Stereological counts through the dorsolateral SVZ of BDNF-GFP NPC-grafted, GFP NPC-grafted, non-grafted lesioned, and non-lesioned mice (n = 4 animals). A significant increase in the number of DCX cells of BDNF-GFP NPC-grafted ($p = 0.010$) and non-grafted, lesioned animals ($p = 0.039$) compared with non-lesioned mice was detected. Transplantation of GFP NPCs also led to an increase in number of DCX cells, but not significantly ($p = 0.124$). Values represent mean ± SEM; *$p < 0.05$, **$p < 0.01$.

affirm these observations with our CatWalk data, as more gait parameters were changed by NPC transplantation in N171-82Q mice than in the R6/2 line. Both mouse models differ in the extent of their neuropathology, life span, and, most importantly, disease progression. Compared with N171-82Q mice, R6/2 animals display a very drastic, accelerative phenotype with a very short life span of 12 weeks, which could hinder cellular survival, proper differentiation, and functional integration after transplantation. In conclusion, toxin-induced lesions, causing massive cell death, serve as the most appropriate HD mouse model for cellular transplantation to date. Even if not optimal in terms of acute cell death, clear positive effects of BDNF NPCs were obtained in the present study. For this reason, we analyzed the mode of action of BDNF NPCs in the QA-lesion model. NPCs expressing either GFP or BDNF-GFP similarly survived grafting, and no differential effect of proliferation was observed. Furthermore, due to the use of MACS purification, no tumor formation was induced by either cell type. Instead, in vivo differentiation was affected in a cell-type-specific manner. BDNF-expressing progenitors mainly differentiated into neurons compared with GFP control cells, which favored glial, and specifically astrocytic lineage differentiation. Enhanced neuronal and GABAergic differentiation by BDNF has been already shown by us and others (Butenschön et al., 2016; Leschik et al., 2013; Ortega and Alcantara, 2010; Trzaska and Rameshwar, 2011). Furthermore, BDNF is known to be an important factor for the postnatal growth of the striatum (Rauskolb et al., 2010) and is essential for the in vitro and in vivo differentiation of striatal neurons (Gokce et al., 2009; Ivkovic and Ehrlich, 1999). Indeed, we found more neurons positive for the striatal marker FOXP1 in BDNF cell grafts than in GFP cell grafts, which underlines the HD therapeutic potential of BDNF NPCs.

FOXP1 labels striatal precursors and differentiated MSNs (Delli et al., 2013). Diverse studies thus far have attempted to pre-differentiate stem cells into transplantable striatal progenitors or MSNs by using various kinds of differentiation protocols. Human ESCs were demonstrated to terminally differentiate into GABAergic DARPP32-positive neurons in vitro and in vivo by the use of sonic hedgehog and BDNF as key molecules (Aubry et al., 2008; Ma et al., 2012). Therefore, our approach with mouse ESCs was to analyze whether very early PSA-NCAM-positive neural progenitors, which expressed one of the earliest telencephalic markers FOXG1, could differentiate in vivo into MSNs through continuous BDNF supply. To obtain NPCs, we used the differentiation protocol of Bernreuther et al. (2006) with minor modifications. This study used mouse ESC-derived L1-overexpressing NPCs in QA-lesioned mice, which led to short-term functional improvement. Here, we show that functional improvement was accompanied by increased striatal differentiation of BDNF NPCs, meaning that BDNF as signaling molecule is sufficient to trigger in vivo differentiation into MSNs. Likewise, for in vitro striatal differentiation of human ESCs, alternatively the potent telencephalic morphogen sonic hedgehog could be used at early stages of differentiation to obtain MSNs after transplantation (Danjo et al., 2011).

In addition to the analysis of in vivo differentiation of transplanted cells, precursor proliferation of endogenous DCX-positive cells was investigated as a potential mechanism leading to improved motor behavior. It is known that striatal QA lesion by itself induces proliferation and migration of adult neuronal stem cells from the dorsal SVZ as an attempt to regenerate the lesioned striatum (Tattersfield et al., 2004). BDNF is known to be an important trigger of adult neurogenesis (Vilar and Mira, 2016). Therefore, transplantation of BDNF-expressing cells could induce a higher migration rate, better survival, increased proliferation, and/or differentiation of SVZ precursor cells. However, we found no difference in the number of DCX-positive cells in QA-lesioned animals with or without BDNF cell transplants, which implies that BDNF exerted no positive effect on endogenous progenitors. Interestingly, GFP transplants significantly reduced the number of DCX cells. In conclusion, this would mean that NPC transplantation by itself induces negative changes in tissue homeostasis or endogenous regeneration, which might be overcome by BDNF. The differences in the motoric outcome after transplantation of both cell types could hence be due to a combination of BDNF-positive effects on differentiation of transplanted cells and its preserving effects on lesion-induced SVZ neurogenesis.

EXPERIMENTAL PROCEDURES

For a more detailed description, see Supplemental Experimental Procedures.

Differentiation of ESCs

V6.5 mouse ESCs were modified by knockin technology into the Rosa26 locus to overexpress either BDNF-GFP or GFP, differentiated into NPCs as described previously with minor modifications, and purified with MACS (Butenschön et al., 2016; Leschik et al., 2013). To ensure cell detection after transplantation, we treated cells with 5 μM BrdU (Sigma-Aldrich) for 48 hr before transplantation.

Cell Transplantation

All experiments were carried out in accordance with the European Union Council Directive of 22 September 2010 (2010/63EU) and were approved by the local animal care committee (Landesuntersuchungsamt Koblenz, permit number G 12-1-097). We transplanted 100,000 cells into the right striatum of QA-lesioned mice and 100,000 cells per striatum bilaterally into R6/2 and N171-82Q mice.

Behavioral Assays

Motor behavior of all mice was tested with the Rotarod, and gait parameters were defined with the CatWalk system. Moreover, QA-lesioned mice were tested with the rotation assay. Both transgenic mouse lines were tested in the open field and grip strength paradigm. Additionally R6/2 mice were tested for clasping performance.

Immunofluorescent Staining

Immunocytochemistry was performed using the following primary antibodies: Nestin, PSA-NCAM, MAP2, OLIG2, KI67, DCX, GFAP, FOXG1, BrdU, and GFP. For immunohistochemistry we used the following antibodies: BrdU, FOXP1, GFAP, S100B, MAP2, BDNF, and GFP. The appropriate secondary Alexa-Fluor antibodies were applied.

SUPPLEMENTAL INFORMATION

Supplemental Information includes Supplemental Experimental Procedures, two figures, and two tables and can be found with this article online at http://dx.doi.org/10.1016/j.stemcr.2016.08.018.

AUTHOR CONTRIBUTIONS

T.Z. designed and performed all experiments and collected datasets. F.R., B.L., and J.L. conceived the study. T.Z., F.R., and J.L. were responsible for the interpretation of results. T.Z. and J.L. wrote the manuscript with the participation of B.L. and F.R. Substantial financial support was given by B.L. All authors read and approved the manuscript.

ACKNOWLEDGMENTS

This work was partly funded by the University of Mainz (Stufe I funding). We thank Andrea Conrad, Ruth Jelinek, and Marcus Keil for excellent technical assistance.

Received: April 13, 2016
Revised: August 31, 2016
Accepted: August 31, 2016
Published: September 29, 2016

REFERENCES

Aubry, L., Bugi, A., Lefort, N., Rousseau, F., Peschanski, M., and Perrier, A.L. (2008). Striatal progenitors derived from human ES cells mature into DARPP32 neurons in vitro and in quinolinic acid-lesioned rats. Proc. Natl. Acad. Sci. USA *105*, 16707–16712.

Bachoud-Levi, A.C., Gaura, V., Brugieres, P., Lefaucheur, J.P., Boisse, M.F., Maison, P., Baudic, S., Ribeiro, M.J., Bourdet, C., Remy, P., et al. (2006). Effect of fetal neural transplants in patients with Huntington's disease 6 years after surgery: a long-term follow-up study. Lancet Neurol. *5*, 303–309.

Behrstock, S., Ebert, A.D., Klein, S., Schmitt, M., Moore, J.M., and Svendsen, C.N. (2008). Lesion-induced increase in survival and migration of human neural progenitor cells releasing GDNF. Cell Transplant. *12*, 753–762.

Bernreuther, C., Dihne, M., Johann, V., Schiefer, J., Cui, Y., Hargus, G., Schmid, J.S., Xu, J., Kosinski, C.M., and Schachner, M. (2006). Neural cell adhesion molecule L1-transfected embryonic stem cells promote functional recovery after excitotoxic lesion of the mouse striatum. J. Neurosci. *26*, 11532–11539.

Buckley, N.J., Johnson, R., Zuccato, C., Bithell, A., and Cattaneo, E. (2010). The role of REST in transcriptional and epigenetic dysregulation in Huntington's disease. Neurobiol. Dis. *39*, 28–39.

Butenschön, J., Zimmermann, T., Schmarowski, N., Nitsch, R., Fackelmeier, B., Friedemann, K., Radyushkin, K., Baumgart, J., Lutz, B., and Leschik, J. (2016). PSA-NCAM positive neural progenitors stably expressing BDNF promote functional recovery in a mouse model of spinal cord injury. Stem Cell Res. Ther. *7*, 11.

Chiang, M., Chen, C., Lee, M., Chen, H., Chen, H., Wu, Y., Hung, C., Kang, J., Chang, C., Chang, C., et al. (2010). Modulation of energy deficiency in Huntington's disease via activation of the peroxisome proliferator-activated receptor gamma. Hum. Mol. Genet. *19*, 4043–4058.

Chiarlone, A., Bellocchio, L., Blazquez, C., Resel, E., Soria-Gomez, E., Cannich, A., Ferrero, J.J., Sagredo, O., Benito, C., Romero, J., et al. (2014). A restricted population of CB1 cannabinoid receptors with neuroprotective activity. Proc. Natl. Acad. Sci. USA *111*, 8257–8262.

Connor, B., Sun, Y., von, H.D., Tang, S.K., Jones, K.S., and Maucksch, C. (2016). AAV-mediated BDNF gene therapy in a transgenic rat model of Huntington's disease. Gene Ther. *23*, 283–295.

Danjo, T., Eiraku, M., Muguruma, K., Watanabe, K., Kawada, M., Yanagawa, Y., Rubenstein, J.L., and Sasai, Y. (2011). Subregional specification of embryonic stem cell-derived ventral telencephalic tissues by timed and combinatory treatment with extrinsic signals. J. Neurosci. *31*, 1919–1933.

Delli, C.A., Onorati, M., Lelos, M.J., Castiglioni, V., Faedo, A., Menon, R., Camnasio, S., Vuono, R., Spaiardi, P., Talpo, F., et al. (2013). Developmentally coordinated extrinsic signals drive human pluripotent stem cell differentiation toward authentic DARPP-32+ medium-sized spiny neurons. Development *140*, 301–312.

Ebert, A.D., Barber, A.E., Heins, B.M., and Svendsen, C.N. (2010). Ex vivo delivery of GDNF maintains motor function and prevents neuronal loss in a transgenic mouse model of Huntington's disease. Exp. Neurol. *224*, 155–162.

El-Akabawy, G., Rattray, I., Johansson, S.M., Gale, R., Bates, G., and Modo, M. (2012). Implantation of undifferentiated and pre-differentiated human neural stem cells in the R6/2 transgenic mouse model of Huntington's disease. BMC. Neurosci. *13*, 97.

Fink, K.D., Rossignol, J., Crane, A.T., Davis, K.K., Bombard, M.C., Bavar, A.M., Clerc, S., Lowrance, S.A., Song, C., Lescaudron, L., et al. (2013). Transplantation of umbilical cord-derived mesenchymal stem cells into the striata of R6/2 mice: behavioral and neuropathological analysis. Stem Cell Res. Ther. *4*, 130.

Foltstein, S.E., Jensen, B., Leigh, R.J., and Foltstein, M. (1983). The measurement of abnormal movement: methods developed for Huntington's disease. Neurobehav. Toxicol. Teratol. *5*, 605–609.

Gallina, P., Paganini, M., Lombardini, L., Mascalchi, M., Porfirio, B., Gadda, D., Marini, M., Pinzani, P., Salvianti, F., Crescioli, C.,

et al. (2010). Human striatal neuroblasts develop and build a striatal-like structure into the brain of Huntington's disease patients after transplantation. Exp. Neurol. *222*, 30–41.

Gauthier, L.R., Charrin, B.C., Borrell-Pages, M., Dompierre, J.P., Rangone, H., Cordelieres, F.P., De Mey, J., MacDonald, M.E., Lessmann, V., Humbert, S., et al. (2004). Huntingtin controls neurotrophic support and survival of neurons by enhancing BDNF vesicular transport along microtubules. Cell *118*, 127–138.

Gokce, O., Runne, H., Kuhn, A., and Luthi-Carter, R. (2009). Short-term striatal gene expression responses to brain-derived neurotrophic factor are dependent on MEK and ERK activation. PLoS One *4*, e5292.

Ivkovic, S., and Ehrlich, M.E. (1999). Expression of the striatal DARPP-32/ARPP-21 phenotype in GABAergic neurons requires neurotrophins in vivo and in vitro. J. Neurosci. *19*, 5409–5419.

Koller, W.C., and Trimble, J. (1985). The gait abnormality of Huntington's disease. Neurology *35*, 1450–1454.

Labandeira-Garcia, J.L., Wictorin, K., Cunningham, E.T., Jr., and Bjorklund, A. (1991). Development of intrastriatal striatal grafts and their afferent innervation from the host. Neuroscience *42*, 407–426.

Landles, C., and Bates, G.P. (2004). Huntingtin and the molecular pathogenesis of Huntington's disease. Fourth in molecular medicine review series. EMBO Rep. *5*, 958–963.

Leschik, J., Eckenstaler, R., Nieweg, K., Lichtenecker, P., Brigadski, T., Gottmann, K., Lessmann, V., and Lutz, B. (2013). Embryonic stem cells stably expressing BDNF-GFP exhibit a BDNF-release-dependent enhancement of neuronal differentiation. J. Cell Sci. *126*, 5062–5073.

Ma, L., Hu, B., Liu, Y., Vermilyea, S.C., Liu, H., Gao, L., Sun, Y., Zhang, X., and Zhang, S.C. (2012). Human embryonic stem cell-derived GABA neurons correct locomotion deficits in quinolinic acid-lesioned mice. Cell Stem Cell *10*, 455–464.

McMurray, C.T. (2001). Huntington's disease. Expanding horizons for treatment. Lancet *358*(Suppl), S37.

Ortega, J.A., and Alcantara, S. (2010). BDNF/MAPK/ERK-induced BMP7 expression in the developing cerebral cortex induces premature radial glia differentiation and impairs neuronal migration. Cereb. Cortex *20*, 2132–2144.

Plotkin, J.L., Day, M., Peterson, J.D., Xie, Z., Kress, G.J., Rafalovich, I., Kondapalli, J., Gertler, T.S., Flajolet, M., Greengard, P., et al. (2014). Impaired TrkB receptor signaling underlies corticostriatal dysfunction in Huntington's disease. Neuron *83*, 178–188.

Ramaswamy, S., McBride, J.L., and Kordower, J.H. (2007). Animal models of Huntington's disease. ILAR. J. *48*, 356–373.

Rauskolb, S., Zagrebelsky, M., Dreznjak, A., Deogracias, R., Matsumoto, T., Wiese, S., Erne, B., Sendtner, M., Schaeren-Wiemers, N., Korte, M., et al. (2010). Global deprivation of brain-derived neurotrophic factor in the CNS reveals an area-specific requirement for dendritic growth. J. Neurosci. *30*, 1739–1749.

Sari, Y. (2011). Huntington's disease: from mutant huntingtin protein to neurotrophic factor therapy. Int. J. Biomed. Sci. *7*, 89–100.

Shin, E., Palmer, M.J., Li, M., and Fricker, R.A. (2012). GABAergic neurons from mouse embryonic stem cells possess functional properties of striatal neurons in vitro, and develop into striatal neurons in vivo in a mouse model of Huntington's disease. Stem Cell Rev. *8*, 513–531.

Snyder, B.R., Chiu, A.M., Prockop, D.J., and Chan, A.W. (2010). Human multipotent stromal cells (MSCs) increase neurogenesis and decrease atrophy of the striatum in a transgenic mouse model for Huntington's disease. PLoS One *5*, e9347.

Tattersfield, A.S., Croon, R.J., Liu, Y.W., Kells, A.P., Faull, R.L., and Connor, B. (2004). Neurogenesis in the striatum of the quinolinic acid lesion model of Huntington's disease. Neuroscience *127*, 319–332.

Trzaska, K.A., and Rameshwar, P. (2011). Dopaminergic neuronal differentiation protocol for human mesenchymal stem cells. Methods Mol. Biol. *698*, 295–303.

Vandeputte, C., Taymans, J.M., Casteels, C., Coun, F., Ni, Y., Van, L.K., and Baekelandt, V. (2010). Automated quantitative gait analysis in animal models of movement disorders. BMC. Neurosci. *11*, 92.

Vilar, M., and Mira, H. (2016). Regulation of neurogenesis by neurotrophins during adulthood: expected and unexpected roles. Front Neurosci. *10*, 26.

Watts, C., and Dunnett, S.B. (1998). Effects of severity of host striatal damage on the morphological development of intrastriatal transplants in a rodent model of Huntington's disease: implications for timing of surgical intervention. J. Neurosurg. *89*, 267–274.

Zuccato, C., and Cattaneo, E. (2009). Brain-derived neurotrophic factor in neurodegenerative diseases. Nat. Rev. Neurol. *5*, 311–322.

Zuccato, C., Marullo, M., Conforti, P., MacDonald, M.E., Tartari, M., and Cattaneo, E. (2008). Systematic assessment of BDNF and its receptor levels in human cortices affected by Huntington's disease. Brain Pathol. *18*, 225–238.

Stem Cell Reports, Volume *7*

Supplemental Information

ESC-Derived BDNF-Overexpressing Neural Progenitors Differentially Promote Recovery in Huntington's Disease Models by Enhanced Striatal Differentiation

Tina Zimmermann, Floortje Remmers, Beat Lutz, and Julia Leschik

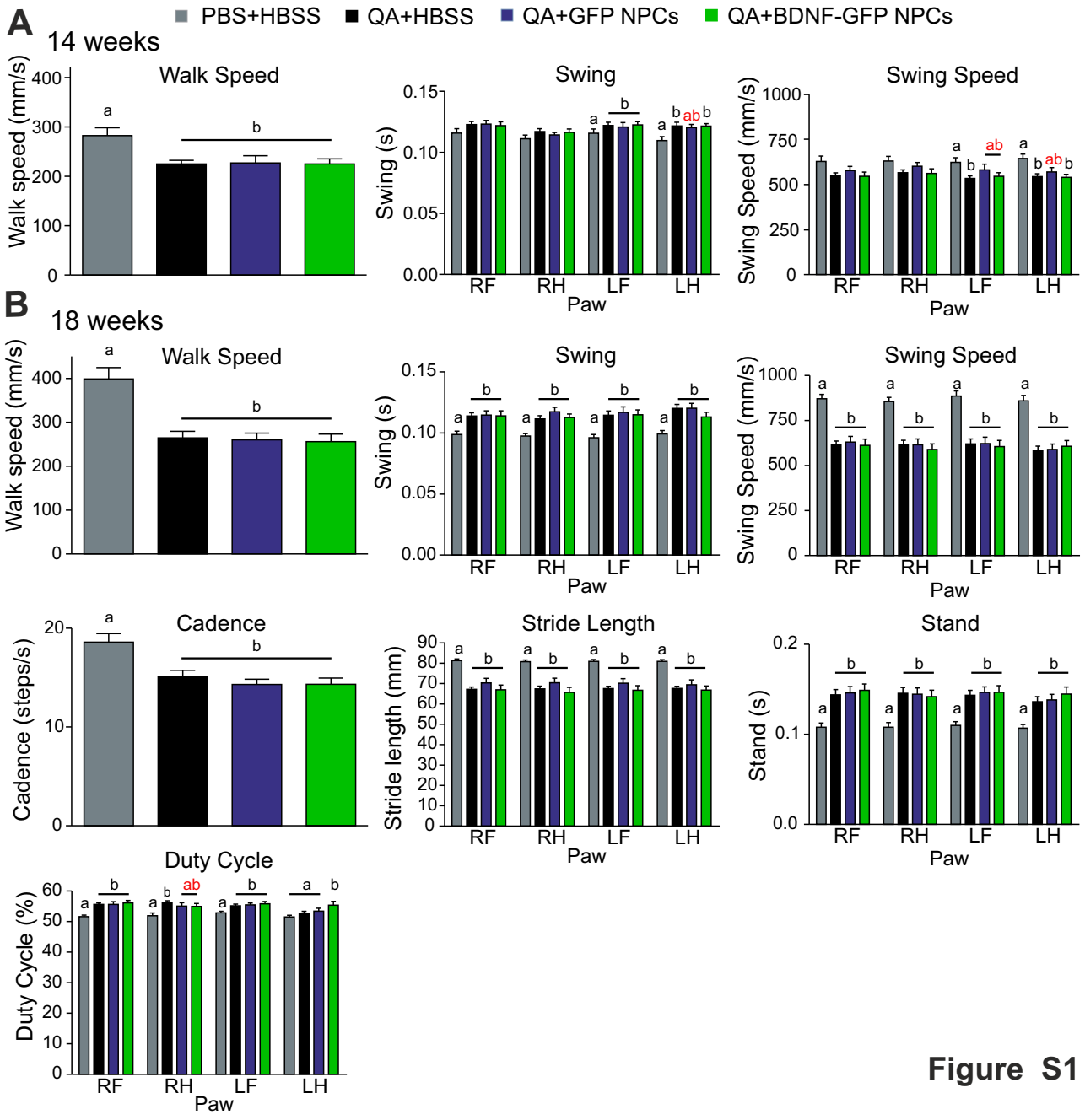
A
PBS+HBSS
QA+HBSS
QA+GFP NPCs
QA+BDNF-GFP NPCs
14 weeks
Walk Speed
Walk speed (mm/s)
Swing
Swing (s)
Swing Speed
Swing Speed (mm/s)
RF
RH
LF
LH
Paw
B
18 weeks
Walk Speed
Swing
Swing Speed
Cadence
Cadence (steps/s)
Stride Length
Stride length (mm)
Stand
Stand (s)
Duty Cycle
Duty Cycle (%)

Figure S1

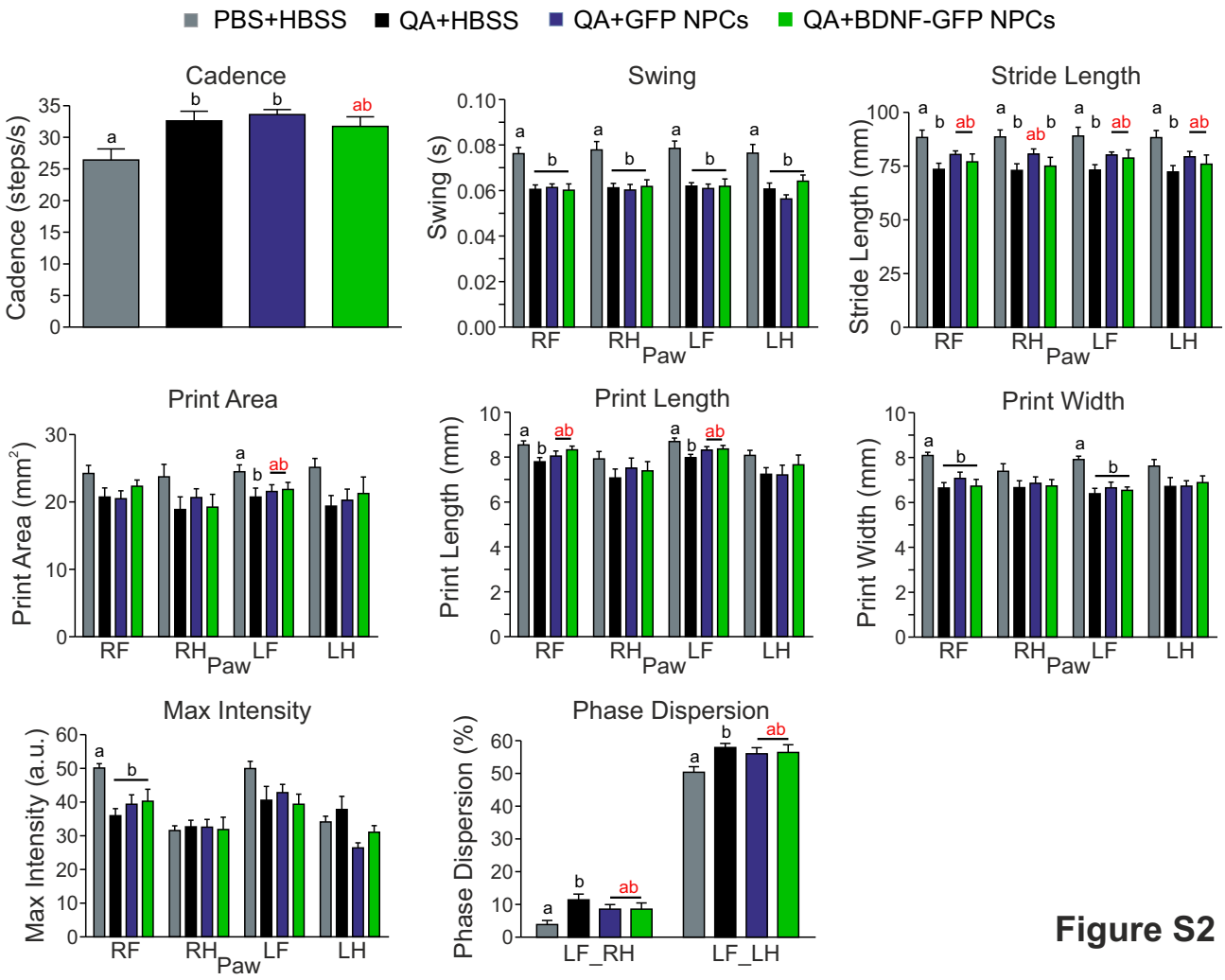
PBS+HBSS
QA+HBSS
QA+GFP NPCs
QA+BDNF-GFP NPCs
Cadence
Cadence (steps/s)
Swing
Swing (s)
Stride Length
Stride Length (mm)
Print Area
Print Area (mm²)
Print Length
Print Length (mm)
Print Width
Print Width (mm)
Max Intensity
Max Intensity (a.u.)
Phase Dispersion
Phase Dispersion (%)
RF
RH
LF
LH
Paw
LF_RH
LF_LH

Figure S2

Supplemental Figure Legends

Figure S1, related to Figure 3. Affected CatWalk parameters of QA lesioned mice. Detailed graphs for the table in Figure 3E. An influence of NPCs can be seen at 14 weeks of age (A) and 18 weeks of age (B). One-way ANOVA with post-hoc Tukey's test between groups for each paw (n=10-12). Data represent mean ± SEM. Values of bars with a different letter (a or b) were significantly different ($p<0.05$) from each other. Values of bars with the same letter (a or b) were not significantly different from each other, hence values of bars marked with "ab" (marked in red) are not significantly different from either a or b, thereby indicating a partial/incomplete rescue of the phenotype. RF= right forepaw, RH= right hindpaw, LF= left forepaw, LH= left hindpaw.

Figure S2, related to Figure 5. Affected CatWalk parameters in the N171-82Q mouse model. Detailed graphs for the table in Figure 5E. Transplanted NPCs had a lasting effect on transgenic compared to wildtype mice. One-way ANOVA with post-hoc Tukey's test between groups for each paw (n=10-12). Data represent mean ± SEM. Values of bars with a different letter (a or b) were significantly different ($p<0.05$) to each other. Values of bars with the same letter (a or b) were not significantly different from each other, hence values of bars marked with "ab" (marked in red) are not significantly different from either a or b, which indicates a partial/incomplete rescue of the phenotype. RF= right forepaw, RH= right hindpaw, LF= left forepaw, LH= left hindpaw.

QA Mouse Model	parameters significant different (p≤0.05)	Paw	PBS+HBSS	QA+HBSS	p vs PBS+HBSS	QA+GFP NPCs	p vs PBS+HBSS	QA+BDNF-GFP NPCs	p vs PBS+HBSS
14 weeks	Walk speed [mm/s]		282.4 ± 16.17	225.3 ± 7.35	p=0.009	227.1 ± 14.89	p=0.018	225.3 ± 10.28	p=0.013
	Swing [s]	LH	0.1095 ± 0.003203	0.1215 ± 0.003048	p=0.018	0.1201 ± 0.00271	p=0.057	0.1214 ± 0.00201	p=0.027
	Swing speed [mm/s]	LF	623.7 ± 25.98	534.7 ± 14.03	p=0.038	582.00 ± 31.69	p=0.109	546.59 ± 19.6	p=0.596
		LH	645.7 ± 24.21	544.4 ± 16.00	p=0.005	570.00 ± 24.96	p=0.067	540.22 ± 17.16	p=0.005
18 weeks	Walk speed [mm/s]		399.0 ± 25.82	264.6 ± 15.08	p=0.0001	259.9 ± 15.65	p=0.0001	255.9 ± 17.36	p=0.0001
	Swing [s]	RF	0.09871 ± 0.0027	0.1138 ± 0.0026	p=0.009	0.1146 ± 0.0034	p=0.005	0.1140 ± 0.0041	p=0.008
		RH	0.09744 ± 0.0019	0.1114 ± 0.0026	p=0.004	0.1179 ± 0.0037	p=0.0001	0.1125 ± 0.0029	p=0.002
		LF	0.09600 ± 0.0027	0.1144 ± 0.0035	p=0.004	0.1169 ± 0.004	p=0.001	0.1148 ± 0.0039	p=0.003
		LH	0.09924 ± 0.0028	0.1201 ± 0.0032	p=0.001	0.1202 ± 0.0040	p=0.0001	0.1131 ± 0.0039	p=0.003
	Swing speed [mm/s]	RF	871.0 ± 24.65	614.0 ± 22.63	p=0.0001	630.4 ± 32.02	p=0.0001	611.8 ± 34.87	p=0.0001
		RH	855.2 ± 23.76	618.3 ± 21.71	p=0.0001	615.7 ± 32.49	p=0.0001	589.2 ± 31.28	p=0.0001
		LF	885.8 ± 28.56	620.6 ± 27.23	p=0.0001	621.9 ± 35.88	p=0.0001	605.7 ± 34.01	p=0.0001
		LH	859.6 ± 30.24	585.7 ± 22.36	p=0.0001	589.4 ± 30.07	p=0.0001	607.3 ± 31.56	p=0.0001
	Cadence [steps/s]		18.6 ± 0.86	15.11 ± 0.62	p=0.005	14.31 ± 0.52	p=0.0001	14.32 ± 0.63	p=0.0001
	Stride length [mm]	RF	81.28 ± 0.7961	67.13 ± 1.185	p=0.0001	70.30 ± 2.267	p=0.0001	66.94 ± 2.310	p=0.0001
		RH	80.73 ± 0.8576	67.37 ± 1.380	p=0.0001	70.39 ± 2.268	p=0.001	65.65 ± 2.505	p=0.0001
		LF	80.91 ± 0.8731	67.55 ± 1.093	p=0.0001	70.18 ± 2.230	p=0.0001	66.72 ± 2.214	p=0.0001
		LH	80.87 ± 0.8301	67.60 ± 1.086	p=0.0001	69.43 ± 2.380	p=0.0001	66.77 ± 2.073	p=0.0001
	Stand [s]	RF	0.1079 ± 0.0047	0.1440 ± 0.0057	p=0.001	0.1461 ± 0.0069	p=0.0001	0.1489 ± 0.0070	p=0.0001
		RH	0.1079 ± 0.0052	0.1456 ± 0.0064	p=0.001	0.1445 ± 0.0070	p=0.001	0.1418 ± 0.0072	p=0.003
		LF	0.1099 ± 0.0042	0.1434 ± 0.0056	p=0.001	0.1467 ± 0.0061	p=0.0001	0.1467 ± 0.0074	p=0.0001
		LH	0.1069 ± 0.0039	0.1363 ± 0.0056	p=0.005	0.1382 ± 0.0062	p=0.003	0.1447 ± 0.0079	p=0.0001
	Duty cycle [%]	RF	51.60 ± 0.5119	55.60 ± 0.4700	p=0.001	55.63 ± 0.92	p=0.001	56.14 0.79	p=0.0001
		RH	51.91 ± 0.8960	56.13 ± 0.6862	p=0.012	55.05 ± 3.54	p=0.088	54.97 ± 3.05	p=0.100
		LF	52.87 ± 0.5117	55.19 ± 0.5481	p=0.049	55.46 ± 0.62	p=0.022	55.82 ± 0.78	p=0.008
		LH	51.51 ± 0.5758	52.65 ± 0.7506	p=0.794	53.43 ± 0.94	p=0.415	55.37 ± 1.25	p=0.017

Table S1, related to Figure 3 and S1. Affected CatWalk parameters of QA lesioned mice. Data represent mean ± SEM. One-way ANOVA with post-hoc Tukey's test between groups for each paw (n=10-12). This table shows exemplarily p-values for all QA-lesioned mice (vehicle and transplanted) compared to non-lesioned mice at 14 weeks of age (4 weeks after transplantation) and 18 weeks of age (8 weeks after transplantation). Values labeled in red are not significantly different to non-lesioned mice, representing the red letter "ab" in Figure S1. This indicates a partial rescue of the phenotype.

Mouse Model	parameters significant different (p≤0.05)	Paw	WT	TG	p vs WT	TG+GFP NPCs	p vs WT	TG+BDNF-GFP NPCs	p vs WT
R6/2	Stride length [mm]	RF	79.95 ± 1.08	71.21 ± 2.53	p=0.015	75.24 ± 1.24	p=0.348	72.38 ± 2.37	p=0.049
		LF	80.46 ± 1.22	71.18 ± 2.59	p=0.014	74.74 ± 1.36	p=0.231	72.97 ± 2.54	p=0.071
		LH	80.86 ± 1.29	70.99 ± 2.57	p=0.006	75.15 ± 1.11	p=0.209	72.62 ± 2.43	p=0.032
	Lateral support [%]		0.55 ± 0.36	5.67 ± 1.94	p=0.041	5.66 ± 0.63	p=0.048	5.43 ± 1.47	p=0.064
N171-82Q	Cadence [steps/s]		26.41 ± 1.75	32.59 ± 1.50	p=0.031	33.59 ± 0.79	p=0.018	31.70 ± 1.53	p=0.069
	Swing [s]	RF	0.0761 ± 0.0027	0.0605 ± 0.0019	p=0.0001	0.0613 ± 0.0015	p=0.002	0.0601 ± 0.0028	p=0.0001
		RH	0.0778 ± 0.0037	0.0611 ± 0.0019	p=0.002	0.0602 ± 0.0024	p=0.002	0.0617 ± 0.0029	p=0.002
		LF	0.0785 ± 0.0032	0.0619 ± 0.0015	p=0.001	0.0609 ± 0.0019	p=0.001	0.0618 ± 0.0032	p=0.0001
		LH	0.0764 ± 0.0039	0.0606 ± 0.0025	p=0.004	0.0562 ± 0.0018	p=0.001	0.0641 ± 0.0027	p=0.026
	Stride length [mm]	RF	88.37 ± 3.39	73.54 ± 2.82	p=0.01	80.46 ± 1.68	p=0.359	77.02 ± 3.71	p=0.058
		RH	88.61 ± 3.25	73.02 ± 3.07	p=0.011	80.64 ± 2.38	p=0.399	75.03 ± 4.05	p=0.025
		LF	89.07 ± 4.06	73.14 ± 2.59	p=0.011	80.24 ± 1.36	p=0.328	78.79 ± 3.84	p=0.139
		LH	88.33 ± 3.29	72.29 ± 2.99	p=0.01	79.34 ± 2.52	p=0.316	75.92 ± 4.25	p=0.054
	Print area [mm²]	LF	24.85 ± 0.98	20.74 ± 1.32	p=0.047	22.16 ± 1.04	p=0.359	22.26 ± 1.01	p=0.304
	Print length [mm]	RF	8.54 ± 0.18	7.79 ± 0.19	p=0.028	8.04 ± 0.22	p=0.286	8.32 ± 0.17	p=0.816
		LF	8.69 ± 0.15	7.97 ± 0.15	p=0.009	8.31 ± 0.15	p=0.358	8.36 ± 0.15	p=0.399
	Print width [mm]	RF	8.09 ± 0.14	6.64 ± 0.24	p=0.001	7.07 ± 0.28	p=0.031	6.73 ± 0.29	p=0.001
		LF	7.91 ± 0.15	6.39 ± 0.24	p=0.0001	6.65 ± 0.26	p=0.001	6.54 ± 0.15	p=0.0001
	Max intensity [a.u.]	RF	50.14 ± 1.29	35.95 ± 2.11	p=0.001	39.38 ± 2.79	p=0.033	40.27 ± 3.55	p=0.030
	Phase dispersion [%]	LF_RH	3.89 ± 1.24	11.43 ± 1.72	p=0.009	8.56 ±1.39	p=0.222	8.57 ± 1.92	p=0.151
		LF_LH	50.39 ± 1.67	57.90 ± 1.28	p=0.029	56.00 ± 1.87	p=0.194	56.44 ± 2.34	p=0.090

Table S2, related to Figures 4, 5, and S2. Affected CatWalk parameters in the R6/2 and N171-82Q mouse model. Data represent mean ± SEM. One-way ANOVA with post-hoc Tukey's test between groups for each paw (n=10-12). This table shows exemplarily p-values for all transgenic mice (vehicle and transplanted) compared to wildtype mice. Values labeled in red are not significantly different to wildtype, representing the red letter "ab" in Figure S2. This indicates a partial rescue of the phenotype.

Supplemental Experimental Procedures

Generation and Differentiation of ESCs

Recombinant ESCs had been obtained by knock-in targeting strategy into the Rosa26 locus. The targeting vector contained the coding sequence of mouse pre-pro-BDNF-GFP (fused to the long 3'UTR of the BDNF gene) or the GFP coding sequence respectively. The ubiquitous CAG promoter (cytomegalovirus enhancer element and the chicken b-actin promoter) was placed upstream of the coding sequence. Furthermore, a floxed-stop cassette was introduced as a transcriptional blocker, which included a neomycin resistance gene. Neomycin resistant target clones obtained after homologous recombination were later transfected with the Cre-Recombinase harboring-vector pCrepac. Then, BDNF-GFP and GFP expressing ESCs were selected with puromycin and clonally expanded. A detailed description of how cells were generated and analyzed has been published by Leschik et al., 2013.
ESCs were maintained on feeder cells (mouse embryonic fibroblasts) and cultured in the presence of leukemia inhibitory factor (LIF). For differentiation, cells were cultured for two passages on gelatin (stage 1) and then differentiated according to the protocol of Bernreuther et al. (2006). This protocol includes embryoid body (EB) formation of ES cells (stage 2), selection of Nestin-positive cells from plated EBs (stage 3) and expansion of Nestin-positive cells (stage 4). Embryoid body formation was induced by plating 2.5 x 10^4 cells/cm² on non-adherent bacterial plastic dishes (Starlab) in ES culture medium without LIF. Embryoid bodies kept in suspension culture for 4 days were plated onto a tissue culture surface (Starlab). On the next day, the medium was switched to ITSFn medium and Nestin-positive cells were selected for 10 days with a medium change every other day. Cells maintained in ITSFn medium were dissociated and replated at a density of 1.5 x 10^5 cells/cm^2 on precoated poly-o/laminin dishes. The expansion medium containing bFGF was changed every 2 days. See a list of ESC culture and differentiation reagents below. After 6 days expansion of Nestin-positive cells, cells were enriched for polysialylated-neural cell adhesion molecule (PSA-NCAM) positive cells and depleted for stage-specific embryonic antigen 1 (SSEA-1) positive cells by MACS (Miltenyi Biotec, Bergisch Gladbach, Germany) as described previously (Butenschön et al., 2016). SSEA-1^-/PSA-$NCAM^+$ sorted cells were plated onto poly-ornithin/laminin coated dishes at a density of 2.0 x 10^5 cells/cm^2 in DMEM/F12/Glutamax supplemented with B27 and differentiated for 3 days by the omission of bFGF.

List of ESC culture and differentiation reagents

Medium	Components	Final concentration	Company	Catalog number
ESC culture medium	DMEM	1x	Sigma	D5671
	FBS	10%	PAA	A15-101
	Non-essential AA	0.1 mM	Invitrogen	11140035
	Sodium Pyruvate	1 mM	Sigma	S8636
	2-Mercaptoethanol	0.1 mM	Sigma	M7522
	L-Glutamine	2 mM	Sigma	G7513
	Pen/Strep	100 U/ml	Sigma	P0781
	LIF	recombinant LIF from supernatant of transfected HEK cells (kind gift from Ari Weissmann)		
ITSFn medium	DMEM/F12 with Glutamax	1x	Invitrogen	10565-018
	Fibronectin	5 µg/ml	Sigma	F2006
	Insulin	5 µg/ml	Sigma	I4011
	Transferrin	50 µg/ml	Sigma	T8158
	Selenium Chloride	30 nM	Sigma	323527
	L-Glutamine	2 mM	Sigma	G7513
	Pen/Strep	100 U/ml	Sigma	P0781
Expansion medium	DMEM/F12 with Glutamax	1x	Invitrogen	10565-018
	bFGF	10 ng/ml	Sigma	F0291
	B27	1x	Invitrogen	17504-044
	L-Glutamine	2 mM	Sigma	G7513
	Pen/Strep	100 U/ml	Sigma	P0781
Gelatin		0.1%	Sigma	1393
Poly-L-ornithine hydrobromide (poly-O)		10 mg/ml	Sigma	P3655
Laminin		5 µl/ml	Sigma	L2020

Animals

Animals were single housed in a temperature- and humidity-controlled room with a 12 h/12 h light / dark cycle (lights on 5 am - 5 pm) and had access to food and water ad libitum. All experiments were carried out in accordance with the European Community's Council Directive of 22 September 2010 (2010/63EU) and were approved by the local animal care committee (Landesuntersuchungsamt Koblenz, permit number G 12-1-097). This study was performed on male C57BL/6J mice (Harlan Laboratories), lesioned with quinolinic acid (Sigma Aldrich), male R6/2 mice (Jackson's laboratories, mouse strain stock number: 002810) and wild-type littermates maintained on the F1 hybrid B6CBA strain and N171-82Q mice (Jackson's laboratories, mouse strain stock number: 003627) and wild-type littermates maintained on the F1 hybrid B6C3H strain. Animals were subjected to genotyping to confirm the presence of the transgene with the mutated huntingtin. CAG repeat sizes were determined from genomic DNA by Laragen Inc. (Culver City, CA). The N171-82Q mice used in this study had a mean CAG repeat length of 84.00 ± 0.06 and the R6/2 mice used in this study a mean CAG repeat length of 167.40 ± 0.91. There was no difference in CAG repeats between transgenic groups. For randomization littermates were split among groups. Experimenters were blind to the genotype of mice and to the treatment.

Quinolinic acid lesion and cell transplantation

Mice were anaesthetized with isoflurane anesthesia and received a subcutaneous injection of buprenorphine (0.05 mg/kg) after the surgery. Mice that were lesioned before the cell transplantation received an additional injection of midazolam (50 mg/kg), to reduce quinolinic acid-induced seizures after waking up from surgery. One week before transplantation, the right striatum (0.0 mm AP, −2.0 mm ML, −3.0 mm DV from bregma) of C57BL6/J mice was lesioned by stereotactic injection of 1 µl 60 nmol quinolinic acid (Sigma, P63204). ESCs, differentiated for 3 days, were trypsinized and resuspended at a concentration of 100,000 cells/µl in HBSS without Ca^{2+} and Mg^{2+} (Gibco, 14175-046). Before transplantation, viability (>95%) of NPCs was validated by Trypan blue exclusion. 1 µl of the cell suspension was injected either in the right striatum of quinolinic acid lesioned mice (same coordinates as for lesioning) or bilaterally in transgenic mice (0.0 mm AP, ±2.0 mm ML, −3.0 DV from bregma) with a flow rate of 500 nl/min with a 26G beveled NanoFil needle. The injection needle was left in place for additional 5 min and then slowly removed. Sham-injected animals received an injection of 1 µl HBSS instead of the cell suspension.

Behavioral assays

All behavioral tests were performed during the light phase of the cycle, starting at 8 am. QA-lesioned and transgenic (R6/2 or N171-82Q) animals had been randomized into treatment groups before transplantation.

Body Weight

Body weight was measured once per week to observe any possible weight loss because of tumor formation of transplanted cells.

Rotation Test

To assess the functional lesion of the right striatum, mice were injected intraperitoneally with apomorphine (Sigma) at a concentration of 2 mg/kg body weight and immediately placed in an acrylic cylinder (20 cm diameter, 25 cm tall) in an Open Field box. The behavior of the mouse was video recorded for 45 min. 5 min after the injection, rotations were counted for 30 min with EthoVision. Net rotations were calculated: number of ipsilateral rotations − number of contralateral rotations.

Rotarod

The rotarod apparatus (Ugo Basile) was used to measure motor coordination and balance. Mice were placed on the rotarod at an accelerating speed ranging from 4 to 40 rpm over 5 min. Mice received three trials per day with a rest period of at least 1 hour in between trials for three consecutive days. On the third day (testing day) the maximum latency to fall off the rotarod for each mouse was recorded. The testing day was repeated every 2 weeks.

Quantitative gait analysis using the CatWalk system

CatWalk XT 9 (Noldus, The Netherlands) was used to assess gait and locomotion. Mice traversed a green illuminated glass plate, the reflected light from the paws that touch the glass was captured with a high-speed video camera and the illuminated paw prints were recorded. The recorded section was 9 mm long and automatic detection settings were applied. The intensity threshold was set to 0.25, the camera gain was set to 37.5. The testing was performed in the dark. Animals were placed on the glass plate and allowed to explore the walkway freely for 3 min. Then the runs were acquired, while the animal was running back and forth voluntarily. The maximum variation was set to 20% and the three fastest trials were used for subsequent analysis.

The following parameters were analyzed (RF= right forepaw, RH= right hindpaw, LF= left forepaw, LH= left hindpaw):

Temporal parameters: walk speed (distance of the runway divided by the time needed to cross), cadence (number of steps per second), stance duration (average time in seconds that the paw is in contact with the glass plate),

swing duration (average time in seconds that the paw is not in contact with the glass plate) and swing speed. Individual paw statistics: maximum contact area, maximum intensity, print area, print width, print length. Comparative paw statistics: stride length (distance between successive placements of the same paw), duty cycle (percentage of time the paw accounts for the total step cycle of the paw), base of support (average distance between front paws or hind paws).

Open Field

Mice were placed in the center of a white box (40 x 40 x 40 cm) illuminated at 90 lux and their behavior was video recorded for 10 min and tracked using EthoVision (Noldus). The distance moved was analyzed.

Grip Strength

To measure forelimb grip strength, a mouse was suspended by the tail and lowered towards the apparatus (Ugo Basile) until it grasped a handle with both front paws. The mouse was pulled back until it released its grip from the handle. All mice were tested for five consecutive trials, the peak pull-force (g) was recorded and the mean pull-force of all five trials was calculated.

Hindlimb Clasping

A marker for disease progression of neurodegeneration in R6/2 mice is hindlimb clasping. Mice were taken by the tail and lifted up in the air for 30 sec (Lee et al., 2009). The foot-clasping time was scored as the following: no clasping equals a score of 0, 0 to 5 sec a score of 1, 5 to 10 sec a score of 2 and more than 10 sec a score of 3.

Immunofluorescent staining

For immunocytochemistry, cells were fixed 15 min with 4% paraformaldehyde (PFA) and washed with PBS. Coverslips were rinsed for 5 min in 0.2% PBS-TX and blocked with 4% goat serum for 20 min. Cells were incubated with primary antibodies in 4% goat serum overnight at 4°C. The second day, coverslips were washed three times 5 min with PBS and incubated with the secondary antibody for 2 h at room temperature. Afterwards, cells were washed, counterstained with DAPI and mounted on (SuperFrostPlus, Menzel, Braunschweig, Germany) slides with Mowiol (Sigma Aldrich).

The following primary antibodies were used: mouse anti-Nestin (1:200), mouse anti-PSA-NCAM (1:100), mouse anti-MAP2 (1:200), mouse anti-OLIG2 (1:1000, all Merck Milipore), rabbit anti-KI67 (1:500), guinea pig anti-DCX (1:500), rabbit anti-GFAP (1:1000) and rabbit anti-FOXG1 (1:500), rabbit anti-BDNF (1:100, all Abcam, Cambridge, UK). Prior to immunostaining with anti-BDNF antibody, antigen retrieval at 98°C in Sodium citrate buffer (10 mM Sodium citrate, 0.05% Tween 20, pH 6.0) was performed. For PSA-NCAM staining, all buffers were used without TX.

For immunohistochemistry, mice were perfused transcardially with PBS followed by 4% PFA, brains were removed, post-fixed overnight in 4% PFA and treated with 30% sucrose for 48 h. Then brains were sectioned 30 µm thick in coronal plane and stored at 4°C in cryoprotection solution until use. Sections were blocked in PBS containing 5% normal donkey serum (NDS), 2.5% BSA and 0.3% TX for 90 min and incubated with the respective primary antibody in PBS containing 1% NDS, 0.1% BSA and 0.3% TX overnight: goat anti-DARPP32 (1:50, Santa Cruz Biotechnologies Inc., Santa Cruz, CA, USA) or guinea pig anti-DCX (1:500, Abcam). For double staining with BrdU, sections were washed 5 min with 0.2% TBS-TX and incubated in 1 N HCl for 1 h at 37 °C to denature DNA, followed by 3 x 5 min washes with TBS. Brain slices were then blocked in TBS with 1% NDS, 0.1% BSA and 0.3% TX for 90 min and incubated with the primary antibodies in blocking buffer overnight at 4°C. On the next day, appropriate secondary antibodies were applied for 2 h. To visualize cell nuclei in non-BrdU treated sections, brain slices were incubated with DAPI for 5 min, washed with PBS and mounted with Mowiol onto slides. The following primary antibodies were used: rat anti-BrdU (1:500), rabbit anti-FOXP1 (1:500), rabbit anti-GFAP (1:1000), rabbit anti-S100B (1:500, all Abcam), rabbit polyclonal anti-MAP2, 1:200 (Merck Milipore), and rabbit anti-ASPA (1:1000, kind gift from Matthias Klugmann, Sydney, Australia).

The respective secondary antibodies were applied: goat anti-mouse IgM or donkey anti-mouse, goat anti-rabbit, goat anti-guinea pig, donkey anti-goat or goat anti-rat AlexaFluor546 and goat anti-mouse, anti-rabbit or anti-rat AlexaFluor647 (all 1:1000; Invitrogen). See a list of all used antibodies below.

List of antibodies

Antibody	Species	Dilution	Company	Catalog number
Nestin	mouse	1:200	Merck Milipore	MAB353
PSA-NCAM	mouse	1:100	Merck Milipore	MAB5324
MAP2	mouse	1:200	Merck Milipore	MAB3418
OLIG2	mouse	1:1000	Merck Milipore	MABN50
KI67	rabbit	1:500	Abcam	ab15580
DCX	guinea pig	1:500	Abcam	ab2253
GFAP	rabbit	1:1000	Abcam	ab7260
FOXG1	rabbit	1:500	Abcam	ab18259
DARPP32	goat	1:50	Santa Cruz	sc-8483
BrdU	rat	1:500	Abcam	ab6326
FOXP1	rabbit	1:500	Abcam	ab16645
S100B	rabbit	1:500	Abcam	ab41548
ASPA	rabbit	1:1000	kind gift from Matthias Klugmann	
anti-mouse IgM AlexaFluor546	goat	1:1000	Invitrogen	A-21045
anti-mouse IgG AlexaFluor546	donkey	1:1000	Invitrogen	A-10036
anti-rabbit IgG AlexaFluor546	goat	1:1000	Invitrogen	A-11010
anti-guinea pig IgG AlexaFluor546	goat	1:1000	Invitrogen	A-11074
anti-goat IgG AlexaFluor546	donkey	1:1000	Invitrogen	A-11056
anti-rat IgG AlexaFluor546	goat	1:1000	Invitrogen	A-11081
anti-mouse IgG AlexaFluor647	goat	1:1000	Invitrogen	A-21235
anti-rabbit IgG AlexaFluor647	goat	1:1000	Invitrogen	A-21244
anti-rat IgG AlexaFluor647	goat	1:1000	Invitrogen	A-21247
Microbeads			**Company**	**Catalog number**
anti-SSEA-1 Micro Beads			Miltenyi	130-094-530
anti-PSA-NCAM-APC Micro Bead Kit			Miltenyi	130-097-859

Microscopic analysis of histology

Slides were observed under a Leica DM5500 (Leica Camera, Wetzlar, Germany) fluorescence microscope or a Zeiss Axiovert LSM 710 (Carl Zeiss, Oberkochen, Germany) laser scanning confocal microscope. For laser scanning confocal microscopy, z-stacks with optical sections of 1 µm of the graft were recorded.
Lesion volume and cell survival were assessed based on the Cavalieri principle of stereology. Lesion size was determined by staining every 10^{th} brain section of the entire striatum of QA-lesioned animals for DARPP32, a medium spiny neuron marker. The lesion area was outlined on digitized images and measured by ImageJ, National Institutes of Health, Bethesda, MD, USA. The lesion volume was calculated by multiplying the distance between sections (300 µm), number of sections and the measured area. Transplanted cells were quantified by staining marked cells with a BrdU antibody. Positive cells were counted in every 6^{th} section (180 µm apart) and calculated for the whole graft. For each parameter four animals were analyzed.
To dissect the differentiation pattern of transplanted cells, BrdU positive cells and BrdU cells positive for the respective cell fate marker were counted in 2 sections of each graft in eight animals per group, analyzing at least 1000 cells per marker and animal.
For evaluation of endogenous precursor proliferation, every 10^{th} brain section was immunostained with DCX and DAPI and positive cells in the ipsilateral dorsolateral subventricular zone (SVZ) were counted.

Statistical Analysis

Data are represented as the mean ± standard error of the mean (SEM). Statistical analysis was done using GraphPad Prism 4 (GraphPad Software Inc, La Jolla, CA, USA) and IBM SPSS Statistics 22v software (IBM Corporation, Armonk, NY, USA). For analysis of behavior over time, analysis of variance (ANOVA) with repeated measures and consecutive Tukey's post hoc tests (for significant group differences) or simple effects

analysis with Sidak correction (for significant group x time interaction) was conducted. The factors were groups x time. Motor behavior at distinct time points was analyzed with one-way ANOVA with post-hoc Tukey's test. For analysis of immunostaining of cells *in-vitro*, two-way ANOVA followed by Bonferroni's corrected multiple comparisons was applied. When comparing only two groups in immunohistology (BDNF-GFP NPCs and GFP NPCs), the two-tailed unpaired Student's t-test was applied. For lesion volume (three groups) and endogenous precursor proliferation (four groups), one-way ANOVA with post-hoc Tukey's or Dunnett's test was used. Differences were assumed to be significant if $p<0.05$.